

Quantum-effective exact multiple patterns matching algorithms for biological sequences

Kapil Kumar Soni and Akhtar Rasool

Department of Computer Science and Engineering, Maulana Azad National Institute of Technology, Bhopal, Madhya Pradesh, India

ABSTRACT

This article presents efficient quantum solutions for exact multiple pattern matching to process the biological sequences. The classical solution takes $O(mN)$ time for matching m patterns over N sized text database. The quantum search mechanism is a core for pattern matching, as this reduces time complexity and achieves computational speedup. Few quantum methods are available for multiple pattern matching, which executes search oracle for each pattern in successive iterations. Such solutions are likely acceptable because of classical equivalent quantum designs. However, these methods are constrained with the inclusion of multiplicative factor m in their complexities. An optimal quantum design is to execute multiple search oracle in parallel on the quantum processing unit with a single-core that completely removes the multiplicative factor m , however, this method is impractical to design. We have no effective quantum solutions to process multiple patterns at present. Therefore, we propose quantum algorithms using quantum processing unit with C quantum cores working on shared quantum memory. This quantum parallel design would be effective for searching all t exact occurrences of each pattern. To our knowledge, no attempts have been made to design multiple pattern matching algorithms on quantum multicore processor. Thus, some quantum remarkable exact single pattern matching algorithms are enhanced here with their equivalent versions, namely enhanced quantum memory processing based exact algorithm and enhanced quantum-based combined exact algorithm for multiple pattern matching. Our quantum solutions find all t exact occurrences of each pattern inside the biological sequence in $O((m/C)\sqrt{N})$ and $O((m/C)\sqrt{t})$ time complexities. This article shows the hybrid simulation of quantum algorithms to validate quantum solutions. Our theoretical-experimental results justify the significant improvements that these algorithms outperform over the existing classical solutions and are proven effective in quantum counterparts.

Submitted 29 July 2021

Accepted 1 April 2022

Published 12 May 2022

Corresponding author

Kapil Kumar Soni,
prof.kapilsoni@gmail.com

Academic editor

Siddhartha Bhattacharyya

Additional Information and
Declarations can be found on
page 51

DOI 10.7717/peerj-cs.957

© Copyright

2022 Soni and Rasool

Distributed under

Creative Commons CC-BY 4.0

OPEN ACCESS

Subjects Bioinformatics, Computational Biology, Algorithms and Analysis of Algorithms, Quantum Computing

Keywords Quantum algorithms, Biological sequences, Grover's quantum search, Quantum memory, Quantum exact multiple pattern matching

INTRODUCTION

The exact multiple pattern matching problem is to find a bijective mapping for m patterns within the text sequence database. Searching for the multiple string patterns would be more practical while processing large biological sequence databases (Basel, 2006;

Neamatollahi, 2020). The search of multiple nucleotides or amino acid patterns is necessary within the genome, protein and other biological sequences for a significant purpose (*Charalampos, Panagiotis & Konstantinos, 2011*). For example, we know that proteogenomics mapping uses proteomics data for DNA or genome annotation. This mapping matches peptide or protein patterns within the proteomics data through the mass spectrometry analysis against the target genome for identifying all locations of genes with coding regions (*Choo, 2006; Fredriksson, 2009*). Therefore, this processing demands a compatible and efficient solution to search for multiple patterns belonging to $P = \{P_1, \dots, P_k, \dots, P_m\}$ with $|P| = m$. Each pattern P_k ($1 \leq k \leq m$) of independent length $M_k = [0 \text{ to } M_k - 1]$ is searched within the large-sized text sequence T of length $N = [0 \text{ to } N - 1]$. Both M and N belongs to the alphabet set Σ such that $N \gg M$, and t number of pattern occurrences is possible to search between index positions 0 and $N - M$. Now, specific to biological sequence processing, we usually prefer these m patterns with the same length. Certainly, the set P contains multiple patterns, although, the restricted singleton set $|P| = 1$ allows us to search P as a single pattern (*Charalampos, Panagiotis & Konstantinos, 2011; Faro & Lecroq, 2013; Zhang et al., 2015; Hendrian et al., 2019; Hakak & Kamsin, 2019*).

The biological sequence database contains N sized text with exponential factors of gigabytes, terabytes or more. For single pattern matching, the classical solution scans these databases in directional sequence on the main memory (*Sheik, Aggarwal & Anindya Poddar, 2004; Kalsi, Peltola & Tarhio, 2008; Rivals, Salmela & Tarhio, 2011*). The search time is still bound to $O(N)$ or the complete scan of text to find all the t occurrences of P ($|P| = 1$); however, for the exponentially large value of N , the problem is computationally hard. Thus, we clarify that the time of pattern search increases in proportion to the size of text database, so fast searching techniques are expected. A classical method for the multiple pattern matching takes $O(mN)$ time complexity due to repeated scanning of N sized text database for m patterns (*Fredriksson, 2009; Charalampos, Panagiotis & Konstantinos, 2011*). In contrast, the quantum search takes $O(\sqrt{N})$ time (*Nielsen & Chuang, 2010*); therefore, a quadratic speedup is possible, and such acceleration is expected in quantum pattern matching (*Soni & Rasool, 2020*). Since the existence of problem, solutions have been suggesting through modified algorithms.

The objective is to suggest effective pattern matching algorithm with better performance than others and to set itself as a benchmark solution. We seek technology-based solutions; therefore, effective quantum-based algorithms are expected for multiple pattern matching. Some quantum-based exact single pattern matching algorithms are enhanced here for their equivalent multiple pattern matching versions (*Soni & Rasool, 2021*). Our methods remove existing multiple pattern matching constraints (*Soni & Malviya, 2021*) and realize the effective quantum-based solutions by scanning the text database in the uniform superposition of quantum memory (QM) (*Giovannetti, Lloyd & Maccone, 2008; Nielsen & Chuang, 2010*). Therefore, based on the advantage of quantum processing unit (QPU) having C quantum cores ($1 \leq c \leq C$) (*Metodi, 2011; Lin et al., 2013; Fu et al., 2016; Britt, 2017; Brandl, 2017*), we propose our algorithms to match m patterns using the quantum-exact match (QEM) circuit (*Sena Oliveira, Benicio Melo de Sousa & Viana*

Ramos, 2007; Soni & Rasool, 2021) and quantum Grover's search operator (GSO) mechanism (Nielsen & Chuang, 2010; Chakrabarty, Khan & Singh, 2017).

Significance of processing biological sequences

For processing the biological sequence databases, exact matches are always preferred with accurate matching outcomes. The nucleotide and amino acid patterns are used to locate within genome, protein and other biological sequences for different purposes (Jiang, Zhang & Zhang, 2013; Singh, 2015). The size of DNA or RNA alphabet set is $|\Sigma| = 4$, and coded adjacent triplet of nucleotide characters which forms amino acid with the set size $|\Sigma| = 20$. The biological sequence databases are excessively large, so multiple string patterns should be effectively processed. Multiple pattern matching aims to identify all locations of m patterns within the sequence databases in a single scan. The searching of DNA pattern within nucleotide sequence helps us to identify, compare and align the sequences as well as to analyze mutations (Faro & Lecroq, 2009; Tahir, Sardaraz & Ikram, 2017; Raja & Srinivasulu Reddy, 2019). However, different nucleotides can code to similar proteins, so protein databases are searched for similarity checks.

An exact multiple pattern matching has more practical applications in computational biology, such as sequence alignments, motif finding, read mapping in gene and genome, substring matching, proteogenomics mapping, overlap detection, codon matching, etc. Thus, the problem is intentionally assumed here to search for the exact occurrences of the patterns (Kalsi, Peltola & Tarhio, 2008; Charalampos, Panagiotis & Konstantinos, 2011; Rivals, Salmela & Tarhio, 2011). There exists an impact of processing large sequences through the efficient algorithm, hence quantum algorithms are made suitable to process biological sequence applications. We search for multiple patterns set $P = \{P_1, \dots, P_k, \dots, P_m\}$ with implicit consideration of processing singleton pattern set to find all t exact occurrence of single nucleotide patterns in gene and genome databases, or multiple nucleotide patterns to confirm the presence of amino acid within the peptide and protein sequences (Singh, 2015; Hakak & Kamsin, 2019). Later, in "proposed algorithmic applications to process biological sequences", we define several applications of our quantum algorithms which are related to searching multiple patterns within the biological sequence databases. For a more comprehensive understanding to process the biological sequences, review these referenced articles (Sheik, Aggarwal & Anindya Poddar, 2004; Basel, 2006; Choo, 2006; Kalsi, Peltola & Tarhio, 2008; Fredriksson, 2009; Charalampos, Panagiotis & Konstantinos, 2011; Rivals, Salmela & Tarhio, 2011; Faro & Lecroq, 2013; Jiang, Zhang & Zhang, 2013; Singh, 2015; Zhang et al., 2015; Tahir, Sardaraz & Ikram, 2017; Hakak & Kamsin, 2019; Neamatollahi, 2020; Soni & Rasool, 2021; Soni & Malviya, 2021; Raja & Srinivasulu Reddy, 2019).

Motivation and contribution of work

The quantum machine can achieve computational speedups because of implicit parallelism. It needs $O(1)$, i.e. constant execution step to realize an exponential number of operations (Nielsen & Chuang, 2010). We assume a problem of pattern matching as hard when the size of text database $N = 2^n$ is excessively large as gigabytes (2^{30}), terabytes (2^{40})

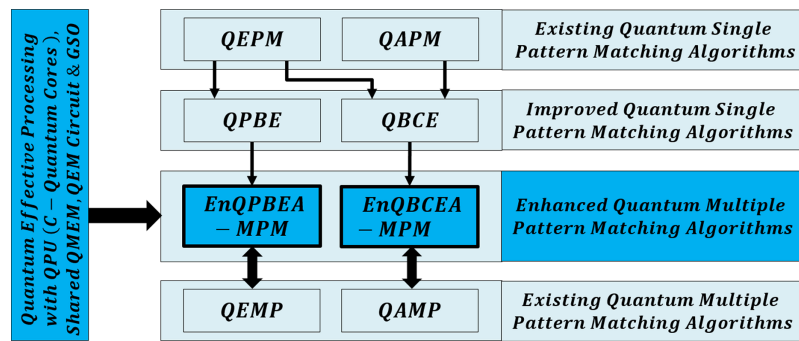


Figure 1 Organization of quantum-based effective multiple pattern matching algorithms.

Full-size DOI: 10.7717/peerj-cs.957/fig-1

or more (Kalsi, Peltola & Tarhio, 2008; Neamatollahi, 2020). So, instead of classical, the quantum pattern search takes reduced $O(\sqrt{N} = 2^n)$ time (Menon & Chattopadhyay, 2021). An existing quantum pattern matching solution achieved speedups over classical complexities (Ramesh & Vinay, 2003; De Jesus, Aborot & Adorna, 2013; Aborot, 2017; Soni & Rasool, 2021); however, the benchmark methods are constrained to find a single pattern, and the quantum multiple pattern matching is found ineffective because of executing multiple search oracles in successive iterations and it includes multiplicative factor m (Soni & Malviya, 2021).

The optimal quantum design may execute multiple search oracle in parallel on QPU with single-core to remove completely such factor m , however, this is impractical to design. We seek exact solutions of pattern matching with more applicability in computational biology. Thus, the available quantum benchmark algorithms QPBE and QBCE are enhanced here, with the names, enhanced QMEM processing-based exact algorithm (EnQPBEA-MPM) and enhanced quantum-based combined exact algorithm (EnQBCEA-MPM) for multiple pattern matching. The design of algorithms is based on processing effectiveness of QPU having C quantum cores and each core shares the text T on QMEM. So, to find all the t exact occurrences of each pattern, the search time complexities of the proposed algorithms are $O((m/C)\sqrt{N})$ and $O((m/C)\sqrt{t})$.

Our motivation is to search for all exact occurrences of m patterns either by direct use of effective quantum processing framework over original text sequence database T in $O(\sqrt{N})$ queries or by transforming approximate filtering outcome into exactness over reduced search space in $O(\sqrt{t})$ queries. The algorithms are based inherently on Grover's search operator (GSO). We use QMEM to explore the text of size $N = 2^n$ such that, the entire text search space is accessed in parallel in $O(1)$ time, but memory word access needs $O(\log_2 N)$ steps (Park & Petruccione, 2019; Matteo, 2020; Soni et al., 2020). A new quantum circuit of $O(1)$ time is proposed for exact match between pattern P and substring of T of size M , whereas classical comparison takes $O(M)$ time (Sena Oliveira, Benicio Melo de Sousa & Viana Ramos, 2007; De Jesus, Aborot & Adorna, 2013; Soni & Rasool, 2021). Thus, we initiate quantum-effective algorithms with a context of exponential increase in biological text size. The proposed work of this article is organized as per Fig. 1, and we derive our results by giving the proofs of Theorem 1 and Theorem 2 in the proposed methods section.

This article presents our main contribution as the effective quantum design of multiple patterns matching algorithms which are proved mathematically along with their simulations. We outline our work below to achieve objectives in a streamlined manner throughout this article:

- We realize the effective quantum processing framework by using QPU with C quantum cores which access quantum processing circuit of equivalent QMEM procedure. It achieves the quantum-based computational and processing speedups. We also proposed, a new constant time, quantum exact match (QEM) circuit which is utilized implicitly under GSO iterations.
- We justify our proposed quantum algorithms using complexities analysis, and specific quantum proving techniques such as probabilistic, truthness and correctness proofs.
- The future works of [Soni & Rasool \(2021\)](#) are presented here as enhanced solutions. Our proposed algorithms EnQPBEA-MPM and EnQBCEA-MPM are proved to search for all t exact occurrence of m patterns with effective time $O((m/C)\sqrt{N})$ and $O((m/C)\sqrt{t})$.
- For a single pattern search, the proposed algorithms EnQPBEA-MPM and EnQBCEA-MPM can simulate the QMEM processing based enhanced designs of QPBE & QBCE algorithms ([Soni & Rasool, 2021](#)).
- A factor (m/C) is proved negligible for a small arbitrary constant value of m and constant value of C as the QPU with C quantum cores utilizing their own set of quantum registers for searching m (m/C) is included explicitly in the time complexities for considering $(m \gg C)$ as the worst case.
- The quantum operations of proposed algorithms are proved equivalent to their quantum circuits. These circuits are the actual realization of quantum solutions. Quantum query, time and storage complexities of proposed algorithms justify their effectiveness.
- Based on several complexity analysis factors, we prove our proposed solutions as efficient to find exact patterns, and these remove the existing multiple pattern matching constraint ([Soni & Malviya, 2021](#)) as designs of QEMP and QAMP cannot exclude multiplicative factor m .
- Our proposed quantum algorithms are simulated for validation through the quantum exact simulation toolkit (QuEST). Also, we proposed a quantum circuit implementation of QMEM through algebraic normal form (ANF). The intentions are not to analyze the efficiency of the simulation due to classical machine restrictions; therefore, we do the hybrid implementation.
- We validate our results using QuEST simulation by assuming that t number of search solutions, either unique or multiple solution, are already known. To realize the case in which the value of t is unknown, we use quantum counting (QC) additionally to validate the search results of our proposed EnQPBEA-MPM and EnQBCEA-MPM algorithms.

- We suggest several applications of EnQPBEA-MPM and EnQBCEA-MPM for processing biological sequences. Such applicability of these algorithms is specified with respect to significant characteristics and performance restrictions.

The abbreviated names used throughout the text are available in Table A1 (Appendix A). The nomenclature used in this article is a prerequisite for further reading purpose, therefore refer to Table B1 (Appendix B). The individual correctness proofs of algorithms EnQPBEA-MPM and EnQBCEA-MPM are separately included in Appendix C and Appendix D. A correctness proof shows algorithmic trace steps which expands the applied quantum operations.

RELATED WORK

Prior work and the important findings

In classical findings, earlier exact multiple patterns matching solutions were proposed as the enhanced version of Knuth–Morris–Pratt (KMP) and Boyer–Moore (BM) algorithms. Both these multiple patterns matching solutions are available in $O(mM)$ time for pattern pre-processing, and searching takes $O(mN)$ (Zhang et al., 2015; Soni & Malviya, 2021). Based on these proposals, other existing algorithms are categorized for multiple pattern matching. There exist several multiple patterns matching methods, few are highlighted with their complexities. Aho–Corasick (AC) is the automata based prefix algorithm that works on KMP logic in $O(m + N)$ time complexity. Commentz–Walter (CW) as a suffix algorithm, extending BM with possible variants, takes $O(m(NM))$ time in worst case. Multiple Pattern Backward DAWG (BDM) and Backward Set Oracle Matching (BSOM) are the factor or substring search-based algorithms which run in $O\left(N\left(\log_{|\Sigma|}(mM)/M\right)\right)$ time (Charalampos, Panagiotis & Konstantinos, 2011; Faro & Lecroq, 2013). Instead, BSOM is a faster method; however, this needs extra space complexity of $O(mM|\Sigma|)$ and verification through the AC algorithm. Wu–Manber (WM) is hashing based algorithm works for a large number of patterns search in $O(N(\lceil M/w \rceil))$ time, where w is number of bits in word size. Shift-OR (SO), Shift-AND (SA), and Backward Non-Deterministic DAWG (BNDM) Matching methods perform bits operation through intrinsic parallelism to realize solutions for multiple patterns matching in $O\left(m\left(N\log_{|\Sigma|}(w)/w\right)\right)$ average time complexity (Fredriksson, 2009; Hendrian et al., 2019). The performance of these algorithms is dependent on $|\Sigma|$, size of text database $|T| = N$, number of patterns $|P| = m$ and each pattern P_k with varying length $M_k = [0 \text{ to } M_k - 1]$. We noted that the multiplicative factor m is somehow included in time complexities of the classical algorithms. Among all the algorithms, AC has significant applications in biological sequence processing. However, AC requires large memory to store the automata, and hence it is constrained to process large patterns set. This algorithm induces competitive results on the small-sized $|\Sigma|$ and $|P| = m$ with each pattern P_k of short length M_k (Fredriksson, 2009; Charalampos, Panagiotis & Konstantinos, 2011; Faro & Lecroq, 2013; Zhang et al., 2015; Hendrian et al., 2019; Soni & Malviya, 2021).

There exist few solutions for quantum pattern matching with the advantage of using amplitude amplification of Grover's search (GSO). This method finds search results over N -sized text in $O(\sqrt{N})$ steps with high probability, and it is better than the classical linear search time $O(N)$ (Lanzogorta & Uhlmann, 2008; Zhou et al., 2013; Coles, 2020). Few single and multiple patterns matching schemes are available in the quantum. Single pattern matching was initiated by Ramesh-Vinay (RV) through the quantum deterministic sampling method; however, the suggested solution needs $O(\sqrt{M} + \sqrt{N})$ time by including the pre-processing and searching (Ramesh & Vinay, 2003; Montanaro, 2017; Menon & Chattopadhyay, 2021). The method quantum approximate pattern matching (QAPM) filters the text for searching a pattern over reduced indices, and it needs $O(t + \sqrt{t})$ (Aborot, 2017). A basic solution of quantum exact pattern matching (QEPM) finds exact leftmost occurrence of the pattern in $O(\sqrt{N})$ time (De Jesus, Aborot & Adorna, 2013). The \sqrt{t} time search is relatively better than \sqrt{N} solution; however, QAPM finds approximate pattern match, and QEPM is constrained to search single pattern occurrence (De Jesus, Aborot & Adorna, 2013; Aborot, 2017).

Recent advancements of these algorithms are presented by extending the logic of QEPM or combining the methods of QEPM and QAPM for effective exact matching design. A suggested QMEM processing based exact (QPBE) algorithm is efficient to process large text sequences and this also overcomes the constraint of QEPM method by finding all t exact occurrences of search pattern in $O(\sqrt{Nt})$ time (Soni & Rasool, 2021). However, the quantum-based combined exact (QBCE) algorithm replaces approximations of the QAPM method with exact matches. This also reduces implicit quantum circuit depth to explore the text during pattern search with logarithmic factors. The desired search time of all t exact occurrence of search pattern is $O(\sqrt{t})$ (Soni & Rasool, 2021). Both these extended solutions are remarkable; however, no attempt has been made yet to design QPBE and QBCE algorithms to process multiple patterns, which are highly expected in biological sequence processing. As well as, the design of QBCE is not available under the specific processing of QMEM (Soni & Rasool, 2021). For quantum multiple pattern matching, initial solutions were suggested as an extension to QEPM and QAPM methods. Soni & Malviya (2021) suggested multiple pattern algorithms, renamed here as quantum exact multiple pattern (QEMP) algorithm to search for either the single occurrence or all t occurrence of m patterns within time complexities range $O(m\sqrt{N})$ and $O(m\sqrt{Nt})$. Rather, renamed quantum approximate multiple pattern (QAMP) search for solution with suggested $O(m(t + \sqrt{t}))$ time. Such algorithms search for the equal and unequal sized patterns in successive iterations, and this includes multiplicative factor m in time complexities. Thus, search solution for multiple pattern algorithms is not effective (Soni & Malviya, 2021).

We are providing the brief description of algorithms QEPM & QAPM, QPBE & QBCE, and QEMP & QAMP from the next subsection onward. As per the reviewed analysis of algorithms, the qubits estimations and algorithmic complexities analysis are also included separately.

Table 1 Analysis of algorithmic complexities QEPM and QAPM algorithms with qubits estimation.

Quantum algorithm	Matching occurrence	Pre-processing complexity	Existing quantum pattern searching time complexity				Storage complexity (qubits estimation)
			Query	Best time	Worst time	Generalized	
QEPM	Single	No Filtering	$O(\sqrt{N})$	$O(\sqrt{N}\log_2 N)$	$O(\sqrt{N}\log_2 N)$	$O(\sqrt{N})$	$O(n + M\log_2 \Sigma)$
QAPM	All	$O(t\log_2 N)$	$O(\sqrt{t}t')$	$O(\sqrt{t}t'\log_2 N)$	$O(t\log_2 N)$	$O(\sqrt{t})$	$O(n + M\log_2 \Sigma + \log_{ \Sigma } M + M)$

Quantum exact pattern matching (QEPM) and quantum approximate pattern matching (QAPM) algorithms

The QEPM method is based on the design of an oracle that performs parallel matching under the quantum superposition by aligning comparison window between pattern and text substring to search for a leftmost exact occurrence of pattern. In $O(\sqrt{N})$ queries, oracle inverts the leftmost index to report pattern match solution with high probability. The algorithm uses GSO and assures $O(\sqrt{N}\log_2 N)$ search time complexity. Table 1 shows that the method is constrained to find a single ($t = 1$) occurrence of pattern, and qubits estimation is the same as quantum search algorithm (De Jesus, Aborot & Adorna, 2013). The algorithm QAPM applies hamming distance (HD) method for approximate text filtering and matching. It cannot find accurate results as HD is an error model and allow replacement at unit cost. A pattern is reported when $HD \leq Threshold$ (pre-computed). A QAPM needs more storage as it uses a large number of quantum registers with excessive qubits requirement (Aborot, 2017); see Table 1. However, this searches all occurrences with $O(\sqrt{t})$ queries. Additional indices may filter using HD, and this increases the size of filtered text, and even HD based verification generates search results with approximation. A filtering needs $O(t\log_2 N)$ time to find all t filtered indices, then verification matches the t' approximate occurrences of pattern through registers comparison, and \sqrt{t} calls of GSO, in the $O(\sqrt{t}t'\log_2 N)$ and $O(t\log_2 N)$ time (Aborot, 2017).

QMEM processing based exact (QPBE) and quantum-based combined exact (QBCE) pattern matching algorithms

The recently proposed algorithms, QPBE and QBCE, are efficient to process the large text sequences. These also overcome the constraints of QEPM and QAPM methods (Soni & Rasool, 2021). The QPBE design is realized efficiently under the superposition of text indices on a quantum memory, and it finds all t exact occurrences of search pattern in $O(\sqrt{Nt})$ time. However, the QBCE algorithm replaces pattern matching approximations with exact matches. It also reduces implicit quantum circuit depth to explore the text during pattern search with the logarithmic factor. A search time for all t' exact occurrences over the reduced text of size t is $O(\sqrt{t}t')$. Both these methods were proposed with significant aspects to process the specific biological sequences. A query remains the same as existing methods, rather the best & worst time complexity of QPBE is $O(\sqrt{Nt}\log_2 N)$ & $O(N\log_2 N)$, and QBCE time complexity is ranging between $O(\sqrt{t}t'\log_2 t)$ and $O(t\log_2 t)$ time. The search oracle for an exact pattern match is found

Table 2 Analysis of algorithmic complexities QPBE and QBCE algorithms with qubits estimation.

Quantum algorithm	Matching occurrence	Pre-processing complexity	Existing quantum pattern searching time complexity				Storage complexity (qubits estimation)
			Query	Best time	Worst time	Generalized	
QPBE	All	NoFiltering	$O(\sqrt{N})$	$O(\sqrt{N}t\log_2 N)$	$O(N\log_2 N)$	$O(\sqrt{N})$	$O(n + M\log_2 \Sigma)$
QBCE	All	$O(t\log_2 N)$	$O(\sqrt{t'})$	$O(\sqrt{t'}\log_2 t)$	$O(t\log_2 t)$	$O(\sqrt{t})$	$O(n + M\log_2 \Sigma + \log_2 t)$

Table 3 Analysis of algorithmic complexities QEMP and QAMP algorithms with qubits estimation.

Quantum algorithm	Matching occurrence	Pre-processing complexity	Existing quantum pattern searching time complexity				Storage complexity (qubits estimation)
			Query	Best time	Worst time	Generalized	
QEMP	Single	No Filtering	$O(m\sqrt{N})$	$O(m(\sqrt{N}\log_2 N))$	$O(m(\sqrt{N}\log_2 N))$	$O(m(\sqrt{N}))$	$O(n + M\log_2 \Sigma)$
	All	No Filtering	$O(m\sqrt{Nt})$	$O(m(\sqrt{Nt}\log_2 N))$	$O(m(N\log_2 N))$	$O(m(\sqrt{N}))$	$O(n + M\log_2 \Sigma)$
QAMP	All	$O(m(t\log_2 N))$	$O(m\sqrt{t'})$	$O(m(\sqrt{t'}\log_2 N))$	$O(m(t\log_2 N))$	$O(m(\sqrt{t}))$	$O(n + M\log_2 \Sigma + \log_{ \Sigma } M + M)$

efficient. As we reviewed, the storage complexity of QPBE is same as the existing QEMP algorithm. The QBCE remarkably reduces the storage while comparing with the excessive qubits requirement of pattern verification used in the existing QAMP method. All the required complexity analysis detail of these algorithms are included in [Table 2](#) for quick reference ([Soni & Rasool, 2021](#)).

Quantum exact multiple pattern (QEMP) and quantum approximate multiple pattern (QAMP) matching algorithms

There are varieties of solutions proposed for the first time on quantum multiple pattern matching. However, the design of such algorithms is based on the execution of search oracle in successive iterations. So for different pattern sizes, it is iteratively called for finding all t occurrence of each pattern P_k . Due to this direct possible design, [Table 3](#) shows that a multiplicative factor (m) is included in the complexities of algorithms ([Soni & Malviya, 2021](#)). The authors categorized multiple patterns matching methods as exact and approximate with quantum memory processing based design. Search complexity of suggested QEMP algorithm to find t occurrence of each P_k ranges between $O((m)(\sqrt{N}t\log_2 N))$ and $O((m)(N\log_2 N))$. In contrast, the QAMP method uses approximate filtering in $O(m(t\log_2 N))$ time to find t filtered indices for each P_k . Further, the iterative search time for each P_k to search all t' occurrences of reduced text of size t , ranges between $O(m(\sqrt{t'}\log_2 N))$ and $O(m(t\log_2 N))$. Both these methods are not increasing storage complexity because of iterative executions; and reasonably, the multiplicative factor m is included. Still, there exist high qubits requirement in the QAMP algorithm (see [Table 3](#)). The time of quantum memory $O(N\log_2 N)$ is considered explicitly due to no such physical availability. These algorithms were suggested to process biological sequences. For the detailed design and analysis of these methods, refer to [Soni & Malviya \(2021\)](#).

QUANTUM ALGORITHMIC FRAMEWORK

Quantum operational framework used in the algorithmic design

Quantum algorithms based on superposition can perform exponential operations in parallel. The quantum behavior realizes qubit presence as $|0\rangle$ and $|1\rangle$ at same time. A $|\psi\rangle$ is a column vector, represents superposition, and $\langle\psi|$ is a row vector; usually, Bra-Ket notation $\langle\psi|\psi\rangle$ is inner product. An n qubits quantum register $|q_i\rangle$ ($q_i \in \{0, 1\}^n$) spans the tensor product of 2^n dimension as Hilbert space. So, the computational basis is formed as $|\psi_n\rangle = \alpha_0|0\rangle + \dots + \alpha_i|i\rangle + \dots + \alpha_{2^n-1}|2^n-1\rangle$ to realize superposition under n dimensional vector space with complex probability amplitudes. Quantum registers can entangle with each other. A measurement collapses superposition into classical states $|i\rangle$ between $|0\rangle$ to $|2^n - 1\rangle$ with probability $|\alpha_i|^2$ such that $\sum_{i \in \{0,1\}^n} |\alpha_i|^2 = 1$. To visualize such n qubits superposition with the required dimensions, refer to these article for the Bloch sphere model ([Choo, 2006](#); [Lanzogorta & Uhlmann, 2008](#); [Nielsen & Chuang, 2010](#); [Coles, 2020](#); [Soni & Rasool, 2020](#)).

Qubits remain in a pure state (vectors), but a quantum gate operator transforms n qubits into $2^n \times 2^n$ sized mixed state (density matrix). The outer product of vectors is obtained as $|\psi\rangle\langle\psi|$ because quantum unitary gate U applies certain operations within superposition to transform the quantum state. A U^\dagger is a conjugate transpose of U that performs the reverse quantum operation, such that $UU^\dagger = I$ holds. Quantum logic operations such as $[H]$ creates superposition, *Pauli* matrices $[X, Y, Z]$ obtains any rotation on Bloch sphere, $[R_x(\theta), R_y(\theta), R_z(\theta)]$ applies rotation with angle θ as unitary operation. Some required controlled operations are $[C^n NOT \text{ or } C^n X]$ which flips the target qubit and $[C^n Z]$ flips the phase of target, when n control qubits are set to 1. The unitary operators encode to perform specific operations under quantum superposition. Refer to Table B1 ([Appendix B](#)) for symbols and used unitary operators throughout this article, and for more comprehensive understanding of quantum operations, refer to the following articles ([Lanzogorta & Uhlmann, 2008](#); [Nielsen & Chuang, 2010](#); [Coles, 2020](#); [Soni & Rasool, 2021](#); [Soni & Malviya, 2021](#)).

Methodology and framework used for quantum algorithm analysis

Our analysis framework for the quantum algorithm is oriented toward quantum-based proof methods. So, we categorized the proofs with their specialized point of interest with their additive use in the quantum algorithmic analysis. We provide the precise description of them as:

- **Quantum Complexity Proof:** The proposed algorithms are justified by using the following complexities analysis. Query complexity shows the number of superposition based oracle calls. Time complexity states the processing time of quantum gates involved in quantum circuits with logarithmic factors. Circuit complexity defines the composition of the quantum circuit with depth. Storage complexity estimates required qubits with ancilla.
- **Quantum Probabilistic Proof:** The proposed algorithms are also proved based on computational theory to identify the quantum complexity class as either the exact

Table 4 Analysis of quantum memory processing, quantum exact match, and quantum search operation.

Quantum design	Quantum algorithmic requirement		Quantum unitary	Quantum time complexity		
	Circuit (gates required)	Storage (qubits required)		Query	Best time	Worst time
QMEM	$C^{n+1}NOT : 1, CNOT : M\log_2 \Sigma $	$O(n + w)$	$U_{QMEM}, U_{Swap}, U_{Load}$	$O(1)$	$O(\log_2 N)$	$O(\log_2 N)$
QEM	$C^2NOT : 3M\log_2 \Sigma $ $C^{\log_2 \Sigma +1}NOT : M, C^{M+1}NOT : 1$	$O(M \times \log_2 \Sigma)$	U_{Comp}	$O(1)$	$O(1)$	$O(1)$
GSO	$H : n + 2n + 1, X : 1 + n + n$ $C^{n+1}NOT : 1, C^nZ : 2$	$O(n + M \times \log_2 \Sigma)$	U_{Mark}, U_{Diff}	$O(\sqrt{N})$	$O(\sqrt{N}\log_2 N)$	$O(N\log_2 N)$

quantum polynomial (EQP) with $Pr = 1$ or bounded error quantum polynomial (BQP) complexity with $Pr = \epsilon$. The probabilistic proof is used to identify results based on probabilities to be used later in lemmas and theorems.

- Quantum Truthness Proof: We prove the algorithms mathematically using Lemma proofs to derive primarily partial results, and then used Theorem proofs to justify the computational complexities result based on rigorous logic and reasoning.
- Quantum Correctness Proof: We proved the proposed algorithms for their correctness on the basis of quantum algorithmic trace steps which expands quantum operations applied under superposition to show quantum state transformations.

(The above-mentioned proofs are categorized on the basis of the following references [Lanzogorta & Uhlmann, 2008](#); [Nielsen & Chuang, 2010](#); [Faro & Lecroq, 2013](#); [Zhou et al., 2015](#); [Broda, 2016](#); [Giri & Korepin, 2017](#); [Grassi, Plasencia & Schrottenloher, 2018](#); [Coles, 2020](#); [Soni & Rasool, 2021](#); [Soni & Malviya, 2021](#)).

Quantum effective processing framework for algorithm design

We generalized a framework for the ordered design of algorithms with (1) processing advantage of quantum memory; (2) proposed efficient quantum exact match (QEM) circuit; and (3) Grover's search to generate high probable results. The remarks of framework are specified in [Table 4](#).

Processing advantage of quantum memory (QMEM)

First, for the compatibility of QPU based computation, both text and pattern are required to encode as quantum data. This facilitates the processing of large biological sequences under quantum superposition. So, QMEM of size $|T_{2^n \times w}\rangle_{QMEM}$ is used to realize superposition with $N = 2^n$ memory words each with size w qubits. The QMEM needs address register $|T_i\rangle_{QA}$ of size $\log_2 N = n$ qubits to refer all text indices $|T_i\rangle_{QA}$ in superposition, and data corresponding to entangled addresses is accessed by data register $|T_{[i]}\rangle_{QD}$ of size $\log_2|\Sigma| = w$ qubits ([Giovannetti, Lloyd & Maccone, 2008](#); [Nielsen & Chuang, 2010](#); [Metodi, 2011](#); [Lin et al., 2013](#); [Fu et al., 2016](#); [Britt, 2017](#)).

The design of QMEM is realized using bucket brigade architecture that enables data access in $O(\log_2 N)$ steps, as among $O(N = 2^n)$ qutrit, $O(\log_2 2^n)$ quantum switch remains active. This design is effective, as classical memory (CRAM) needs all $O(N = 2^n)$ switches active for word access. So, QMEM gains exponential speedup as $(2^n / \log_2 2^n)$ over

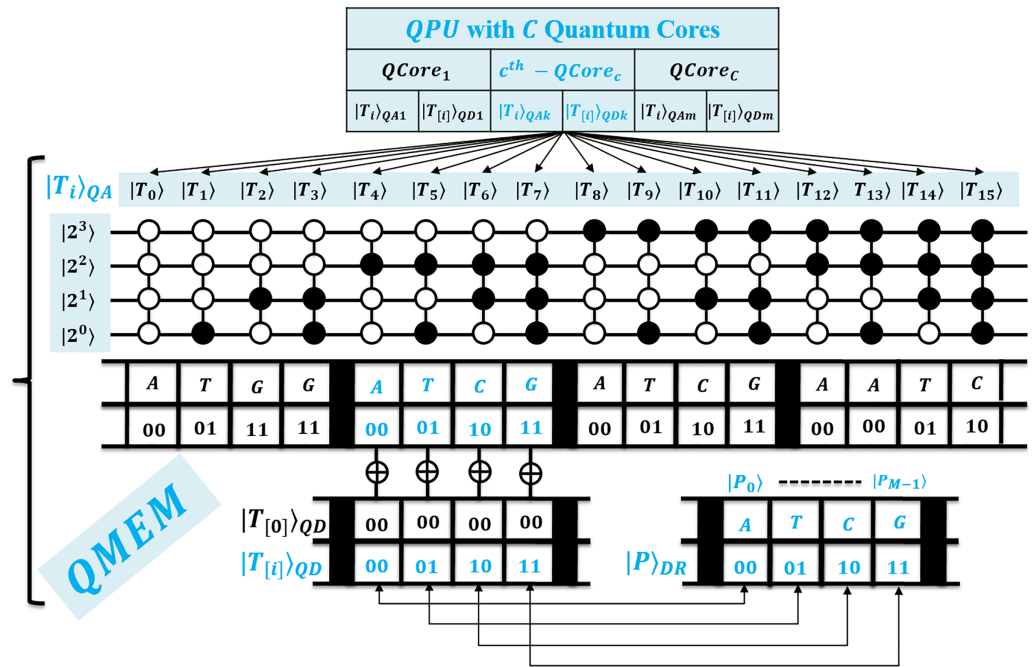


Figure 2 Quantum circuit equivalent to the quantum memory (QMEM) processing.

Full-size DOI: 10.7717/peerj-cs.957/fig-2

CRAM. A text is shared on memory, and each c^{th} core $QCore_c$ can access it in owned superposition. A QPU with C cores uses their registers set, and such parallelism minimizes processing time as negligible. Figure 2 shows the architecture of QPU with C cores working on shared QMEM with the design of the quantum memory circuit. A QMEM is realized using U_{QMEM} of Eq. (1) in support of Eqs. (2)–(4) (Giovannetti, Lloyd & Maccone, 2008; Nielsen & Chuang, 2010; Metodi, 2011; Lin et al., 2013; Fu et al., 2016; Britt, 2017; Brandl, 2017; Park & Petruccione, 2019; Matteo, 2020; Soni et al., 2020).

$$\text{QMEM Transformation} \leftarrow (U_{\text{QMEM}} \leftarrow (U_{\text{Swap}}^\dagger (U_{\text{Load}} (U_{\text{Swap}})))) \quad (1)$$

$$U_{\text{Swap}}(|0\rangle|\text{wait}\rangle) = |f\rangle|\text{left}\rangle \text{ or } U_{\text{Swap}}(|1\rangle|\text{wait}\rangle) = |f\rangle|\text{right}\rangle \quad (2)$$

$$U_{\text{Load}}(|T_i\rangle_{\text{QA}} \otimes |T_{[w]} \rangle_{\text{QD}}) = U_{\text{Load}}(|T_i\rangle_{\text{QA}} \otimes |T_{[w \oplus i]} \rangle_{\text{QD}}) = |T_i\rangle_{\text{QA}} \otimes |T_{[i]} \rangle_{\text{QD}} \quad (3)$$

$$U_{\text{Swap}}^\dagger(|f\rangle|\text{left}\rangle) = |0\rangle|\text{wait}\rangle \text{ or } U_{\text{Swap}}^\dagger(|f\rangle|\text{right}\rangle) = |1\rangle|\text{wait}\rangle \quad (4)$$

A unitary U_{QMEM} makes the data available in parallel for each $|T_i\rangle_{\text{QA}}$ index. It prepares the $|\text{qutrits}_{N-1}\rangle$ switches in $|\text{wait}_{N-1}\rangle$ state and realizes the superposition of entire memory. As per target index $|T_i\rangle_{\text{QA}}$, the qutrit are transformed from $|\text{wait}\rangle$ to $|\text{left}\rangle$ or $|\text{right}\rangle$ state using U_{Swap} of Eq. (2) under fiduciary qubit $|f\rangle$ that fixes switch state. Among $|\text{qutrits}_{N-1}\rangle$ only the $|\text{qutrits}_{\log_2 N}\rangle$ remains active during the memory call [14]. We perform the data loading using U_{Load} of Eq. (3). It activates bus qubits to trace a path of active qutrit switches, copies the cell data, and traces back over same qutrit to load copied data into $|T_{[i]} \rangle_{\text{QD}}$, and meanwhile, qutrit are transformed to $|\text{wait}\rangle$ state by reverse unitary U_{Swap}^\dagger of Eq. (4) (Giovannetti, Lloyd & Maccone, 2008; Nielsen & Chuang, 2010).

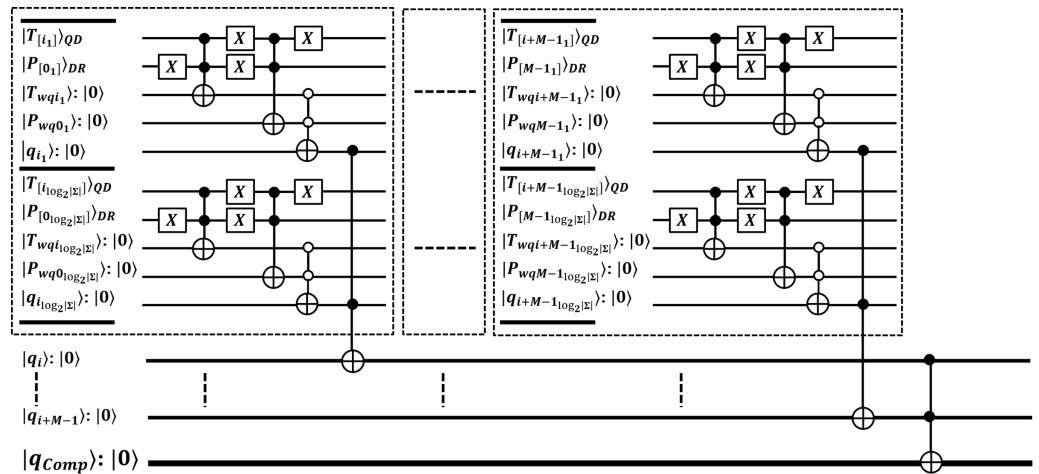


Figure 3 Quantum circuit for exact pattern match as (QEM) working with QMEM processing.

Full-size [DOI: 10.7717/peerj-cs.957/fig-3](https://doi.org/10.7717/peerj-cs.957/fig-3)

A QMEM needs $O(\log_2 N)$ steps; and a memory call enables the bus qubits equal to the word size to access data in parallel, so for $w = M \times \log_2 |\Sigma|$ qubits, the $\log_2 N$ switch remains active until the word transfer is not completed. Therefore, with word transfer, the QMEM needs $O(M \times \log_2 N)$ steps with the negligible factor M (Nielsen & Chuang, 2010; Soni et al., 2020; Soni & Rasool, 2021; Soni & Malviya, 2021).

Proposed efficient quantum exact match (QEM) circuit

Second, we propose quantum-exact match (QEM) circuit through unitary U_{Comp} to perform parallel match between pattern $|P_{[0 \text{ to } M-1]}\rangle_{DR}$ and retrieved substring in register $|T_{[w]}\rangle_{QD}$ of size $w = M \times \log_2 |\Sigma|$ qubits. We seek an exact match on behalf of each index $|T_i\rangle_{QA}$ in superposition on QMEM. This circuit compares the qubits of size $\log_2 |\Sigma|$ for each symbol contained in $|P\rangle_{DR}$. So, for M length pattern, all $\log_2 |\Sigma|$ sized qubits are analyzed in $O(1)$ time. We specified the QEM operation in Eq. (5), and relevant circuit is shown in Fig. 3 with depth 2 i.e. $O(1)$ (Sena Oliveira, Benicio Melo de Sousa & Viana Ramos, 2007; De Jesus, Aborot & Adorna, 2013; Soni & Rasool, 2021; Soni & Malviya, 2021).

$$\text{QEM Operation} \leftarrow \left(U_{Comp} : f(|T_i\rangle_{QA}) = \begin{cases} 0, & \text{if } |T_{[i \text{ to } i+M-1]}\rangle_{QD} \neq |P_{[0 \text{ to } M-1]}\rangle_{DR} \\ 1, & \text{if } |T_{[i \text{ to } i+M-1]}\rangle_{QD} = |P_{[0 \text{ to } M-1]}\rangle_{DR} \end{cases} \right) \quad (5)$$

The comparison between $|P_{[0 \text{ to } M-1]}\rangle_{DR}$ and $|T_{[i \text{ to } i+M-1]}\rangle_{QD}$ is performed by unitary U_{Comp} in an explored superposition of QMEM with text indices $|T_i\rangle_{QA}$. So, entire $w = M \times \log_2 |\Sigma|$ qubits sized substring is compared in parallel with constant time. This circuit is designed with $3 \times M \times \log_2 |\Sigma| = C^2 NOT$ gates which are arranged at level zero (for M sized text substring and pattern, and M additional ancilla). At level one, we used $M = C^{\log_2 |\Sigma|+1} NOT$ gates to check for equality as either $|0\rangle == |0\rangle$ or $|1\rangle == |1\rangle$ between aligned qubits of size $\log_2 |\Sigma|$ for each character of P . Last level is designed with single $C^{M+1} NOT$ gate that flips a target qubit $|q_{Comp}\rangle$ to indicate the quantum-based

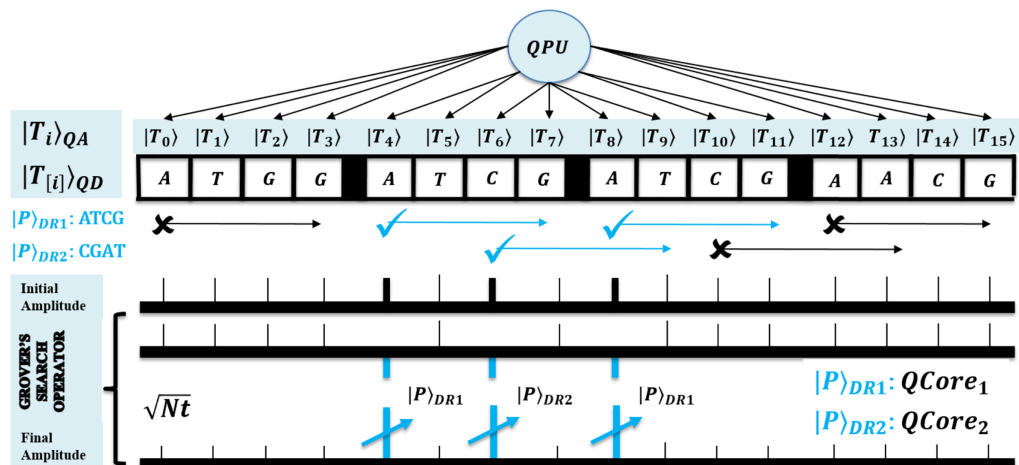


Figure 4 Quantum-based illustration of the EnQPBEA-MPM algorithm.

Full-size DOI: 10.7717/peerj-cs.957/fig-4

exact match. So, the depth of quantum circuit is $O(1)$. The qubits requirement of the proposed circuit is $(3 \times M \times \log_2|\Sigma|) + M + 1$ and we estimate asymptotic complexity with $O(M \times \log_2|\Sigma|)$. Thus, this quantum-exact match (QEM) circuit is efficient.

Grover's search operator (GSO) to generate high probable results

Third, Grover's method is optimal to search for pattern in $O(\sqrt{N})$ steps over N size text. It uses amplitude amplification that repeats for $\pi/4\sqrt{N}$ times, each iteration applies reflection operations for transforming target index to high amplified amplitude under superposition state, and thus to obtain high probable search results (Nielsen & Chuang, 2010; Chakrabarty, Khan & Singh, 2017). So, $O(\sqrt{N})$ steps assure to eventually result in the desired state with significantly large amplitude. A method is shown in Fig. 4 and it's next to next figure. No more iterations than \sqrt{N} is recommended, as this succeeds with a solution on the sine function principle. It gradually increases as per the increase in function argument, but later this starts decreasing. However, this search mechanism is the only way to achieve a quadratic speedup (Lanzogorta & Uhlmann, 2008; Zhou et al., 2013; Coles, 2020).

The GSO operation is defined as Eq. (6) with sub-unitary specified in Eqs. (7) and (8). A search oracle $O \leftarrow (U_{\text{Mark}}(U_{\text{Comp}}))$ marks the target index location of the pattern when U_{Comp} of Eq. (5) is succeeded for the exact match through Boolean oracle. Further, phase inversion is applied by phase oracle using $U_{\text{Mark}}(|T_i\rangle_{\text{QA}} \otimes |q\rangle)$ of Eq. (7) to reflect the target index amplitude as $|T_i\rangle_{\text{QA}}|-\rangle \rightarrow (-1)^{f(|T_i\rangle_{\text{QA}})}|T_i\rangle_{\text{QA}}|-\rangle$. Another reflection operator diffusion $D \leftarrow (U_{\text{Diff}}(O))$, defined in Eq. (8), inverts all amplitudes around the mean, such that the amplitude of solution increases and the others decrease. In actual, this method amplifies the search index amplitude in each iteration (Lanzogorta & Uhlmann, 2008; Zhou et al., 2013; Broda, 2016; Giri & Korepin, 2017; Figgatt et al., 2017; Coles, 2020). The GSO operational description is provided in correctness proof of proposed algorithms.

$$\text{GSO Operation} \leftarrow (D \leftarrow U_{\text{Diff}}(O \leftarrow (U_{\text{Mark}}(U_{\text{Comp}})))) \quad (6)$$

$$\begin{aligned} O \leftarrow U_{\text{Mark}}(|T_i\rangle_{\text{QA}} \otimes |q\rangle) &= (I - 2|T_i\rangle_{\text{QA}}\langle T_i|_{\text{QA}}) \otimes (|T_i\rangle_{\text{QA}} \otimes |q\rangle) \\ &= \begin{cases} |T_i\rangle_{\text{QA}}, & f(|T_i\rangle_{\text{QA}}) = 0 \\ -|T_i\rangle_{\text{QA}}, & f(|T_i\rangle_{\text{QA}}) = 1 \end{cases} \end{aligned} \quad (7)$$

$$D \leftarrow U_{\text{Diff}}(O) = D((2|\psi_n\rangle\langle\psi_n| - I)(O)) = D(H^{\otimes n}(2|0\rangle\langle 0| - I)H^{\otimes n}(O)) \quad (8)$$

A GSO works under superposition state $|\psi_n\rangle$ by making an angle $(\pi/2 - \theta)$ and transforms the solution state by applying each time 2θ rotations. So, for r rotations, $(r \times 2\theta = \pi/2 - \theta)$ then $(r = \pi/4\theta - 1/2)$. In superposition of N elements, the amplitude for each of t solutions are $\sqrt{t/N}$, so $\theta = \sqrt{t/N}$. On U_{Comp} success $Pr[\text{GSO outputs } |T_i\rangle_{\text{QA}} \text{ if } f(|T_i\rangle_{\text{QA}}) == 1] = t/N$. So, put this phase θ in r we get $(r = \pi/4\sqrt{N/t} - 1/2) \approx \pi/4\sqrt{N/t} \cong O(\sqrt{N/t})$ step. For geometric proof, refer (Nielsen & Chuang, 2010; Broda, 2016; Chakrabarty, Khan & Singh, 2017; Coles, 2020; Soni & Rasool, 2021; Soni & Malviya, 2021). The $1 \leq t \leq N$ solutions are searched in $\sqrt{N/t}$ query and $O(\sqrt{N/t} \log_2 N)$ time with $Pr[\text{GSO outputs } |T_i\rangle_{\text{QA}} \text{ if } f(|T_i\rangle_{\text{QA}}) == 1] \geq t/N$.

As reviewed, analysis of quantum effective processing framework is specified in Table 4. The QMEM makes searching outcomes available in parallel with $O(1)$ step. The unitary U_{Comp} of $O(1)$ time is used in GSO as implicit operation and it is simulated on QMEM design. The GSO can find number of pattern occurrences $t = t_{\text{few}}$ (multiple solution), where t_{few} denotes few pattern occurrences ($t_{\text{few}} \ll N$), using $O(\sqrt{N/t})$ queries and $O(\sqrt{N/t} \log_2 N)$ time. As $H^{\otimes n}$ operations run in parallel, each with $O(1)$ time, so asymptotic complexity is considered as $O(\sqrt{N/t})$ with respect to negligible multiplicative factor $(\log_2 N)$ (Brassard et al., 2002; Lomont, 2003; Ablayev et al., 2020). If it is known that the $t = 0$ (no solution), then GSO returns a random element uniformly in $O(\sqrt{N})$ time. In case, $t = 1$ (unique solution), search result can be obtained in $O(\sqrt{N})$ time with high probability.

To report t search solution, GSO needs $t \times \sqrt{N/t} = \sqrt{t} \times \sqrt{t} \times \sqrt{N/t} = \sqrt{Nt}$ queries and $O(\sqrt{Nt} \log_2 N)$ time. However, all solutions $t = 1$ or t_{few} are possible in $O(\sqrt{N})$ and when $t = N$ (all are search solution), the search time is $O(N)$ i.e. same as the classical. For $t = 1$ case, GSO can obtain the result with high probability after \sqrt{N} iterations, however, more \sqrt{N} iterations can again generate uniform probability. This may happen repeatedly in each successive \sqrt{N} iterations. Therefore, only $O(\sqrt{N})$ iterations are needed to obtain high probable search solution. We prefer the quantum search to find the few pattern occurrences. The consideration of $t = N$ is found rare for a biological text, and hence this can be ignored (Nielsen & Chuang, 2010; Broda, 2016; Chakrabarty, Khan & Singh, 2017; Soni & Rasool, 2021; Soni & Malviya, 2021).

To our knowledge, the quantum search assumes that the number of search solutions t (either unique or multiple solution) are already known. Therefore, number of GSO iterations can be determined in advance and after $\pi/4\left(\sqrt{N/t}\right)$ iterations the search results are found with certainty and high probability. However, the GSO can overshoot if the t number of search solutions are unknown/not known in advance. In that case, with the unknown number of GSO iterations, the probability of success would be vanishingly small (Boyer et al., 1998; Brassard et al., 2002; Lomont, 2003; Younes, 2008; Song, 2017; Ablayev et al., 2020).

To deal with the unknown number of search solutions, one of the methods was proposed by Boyer et al. (1998) and restated in Younes (2008); Song (2017) and Ablayev et al. (2020) as the modified Grover's search that runs GSO several times in successive iterations. The modified algorithm of Boyer et al. (1998) repeats GSO by taking the value of t in an exponential increase. On j^{th} repetition, $\pi/4\left(\sqrt{N/2^j}\right)$ iterations are performed. The repetitions are here summing to $O(\sqrt{N})$ times. Either of these iterations may find the search results with a sufficient high probability. In each of these repetition, the GSO operations are still bounded by $\pi/4(\sqrt{N})$ iterations. It is equivalent to $O(N)$ time classical complexity, so not used in practical implementation (Boyer et al., 1998).

Quantum counting (QC) is an alternative approach that can satisfactorily handle the problem of unknown number of search solutions (Brassard et al., 2002; Lomont, 2003; Song, 2017). A QC is quantum amplitude estimation (QAE) method that can estimate t number of search solutions either based on approximation or based on exactness. It helps to decide the required number of GSO iterations. The QAE technique is defined in Brassard et al. (2002) and Fang Song (2017), and it is used for estimating

$t = \left| \left\{ |T_i\rangle_{\text{QA}} \in N \mid f(|T_i\rangle_{\text{QA}}) = 1 \right\} \right|$ as the possible count to find the number of search solutions. These authors (Boyer et al., 1998; Brassard et al., 2002; Lomont, 2003) suggested to run quantum counting algorithm initially, and then to proceed with actual number of GSO iterations. Quantum counting results can be obtained with quadratic speedup in $O(\sqrt{N})$ time. Therefore, we observed it as an efficient method when the number of search solutions are unknown, and hence it prevents overshooting of Grover's. Later, in theoretical results and complexity analysis section, we analyze the exact and approximate quantum counting methods, and these are implemented to simulate our algorithms.

A circuit of QMEM needs $C^{n+1}NOT$ to mark $|T_i\rangle_{\text{QA}}$ address, and to store $w = M \times \log_2|\Sigma|$ in $|T_{[w]}\rangle_{\text{QD}}$ we use $M \times \log_2|\Sigma| = CNOT$. This memory is exponentially faster than the CRAM circuit. However, its access depends on the depth of the bifurcation tree i.e. $O(\log_2 N)$ time. Quantum search works with QMEM by applying $H^{\otimes n}(|T_i\rangle_{\text{QA}})$ and $XH(|q\rangle)$ and then U_{Comp} checks for exact match followed by amplification. On a successful match, qubit $|q\rangle$ is flipped by $C^{n+1}NOT$ gate, then U_{Mark} flips the phase of index $|T_i\rangle_{\text{QA}}$ by C^nZ gate. Diffusion performs the amplification through the set of quantum operators $\{ \{ H^{\otimes n} X^{\otimes n} \} C^n Z \{ H^{\otimes n} X^{\otimes n} \} \}$. At the last, perform measurement at index $|T_i\rangle_{\text{QA}}$. In addition, we included qubits requirement for QMEM and GSO. Quantum gates and the circuit requirement of the framework is shown in Table 4. However, our remark states that quantum search over text T of size N takes $n + 2M\log_2|\Sigma| + 1$ qubits (Lanzogorta &

Uhlmann, 2008; Nielsen & Chuang, 2010; Zhou et al., 2013; Broda, 2016; Chakrabarty, Khan & Singh, 2017; Giri & Korepin, 2017; Figgatt et al., 2017; Coles, 2020; Soni & Rasool, 2021; Soni & Malviya, 2021). Further, n is replaced by tq qubits for the search which is performed over the reduced size filtered text. A QMEM is efficiently simulated using algebraic normal form (ANF) for the hybrid realization of quantum operations (*Bogdanova et al., 2018; Malviya & Tiwari, 2020; Hao et al., 2020; Malviya & Tiwari, 2021*).

THE PROPOSED METHODS

This section includes proposed EnQPBEA & EnQBCEA algorithms. Both these designs use the effective quantum processing framework. Algorithms can process multiple patterns string of set $P = \{P_1, \dots, P_k, \dots, P_m\}$ with each pattern P_k of length M_k ($1 \leq k \leq m$), using the shared text T of size N explored on QMEM to search all exact match occurrence of individual pattern $P_k \in P$ through c^{th} core $QCore_c$ of QPU having C quantum cores. Our algorithms are enhancement of improved QPBE & QBCE methods for processing multiple patterns with an aim to remove the multiplicative factor m in complexities. The proposed solutions are remarkable and efficient on comparing with existing QEMP & QAMP multiple pattern methods. We modify the design of algorithms by running multiple search oracles in parallel. A QPU runs C cores to search for m/C pattern in parallel, and each quantum core uses its own set of registers. So a multiplicative constant (m/C) with a small arbitrary constant value of m and constant value of C is found negligible. However, for comparatively large value of $m \gg C$, a factor m/C cannot be ignored in the complexities analysis. Hence, we initially clarify that for few pattern occurrences, the storage and time both are implicitly saved in enhanced designs of algorithms. We justify our proposed methods by giving the proof of the resulting Theorems 1 and 2. Later, we show the efficient and effective hybrid simulation of these quantum algorithms.

Proposed method 1: enhanced QMEM processing based exact algorithm for multiple pattern matching (EnQPBEA-MPM)

This method searches for each pattern $P_k \in P$ in parallel using QPU with C cores accessing text T on shared QMEM, such that search time of all t_k occurrence of P_k overlaps. QEM circuit is applied under superposition of text on QMEM by each $QCore_c$. Search results are instantly possible and would be effective for the biological sequencing because of no other processing overhead except the search time. Existing QPBE is enhanced efficiently by executing search oracles in parallel with the negligible time factor, and the existing iterative pattern search overhead of QEMP is also removed.

A pattern $P_k \in P$ is individually processed on c^{th} core $QCore_c$ where ($1 \leq c \leq C$), so m/C patterns are searching in parallel within the text T of size N shared on QMEM. Each pattern P_k is assumed with individual size $w = M_k * \log_2|\Sigma|$ qubits, and it is stored in $|P_{[0 \text{ to } M_k-1]}\rangle_{DRk}$ as in separate data register. The text T realized on $|T_{2^n \times w}\rangle_{QMEM}$ is accessed in a superposition of addresses by $QCore_c$ through address register $|T_i\rangle_{QAk}$ ($i \in \{0, 1\}^n$). All the text substrings, each of length $M_k * \log_2|\Sigma|$ are loaded in entangled register $|T_{[w]}\rangle_{QDk}$ by applying QMEM transformation. A unitary U_{Load} makes sure such data load

Proposed Algorithm 1: EnQPBEA-MPM.

- Data : Text T stored on $|T_{2^n \times w}\rangle_{\text{QMEM}}$ which is accessed by quantum registers $\{|T_n\rangle_{QA1}, \dots, |T_n\rangle_{QA_m}\}$ and $\{|T_{[w]}\rangle_{QD1}, \dots, |T_{[w]}\rangle_{QD_m}\}$, the implicit data registers $\{|P_{[0 \text{ to } M_1-1]}\rangle_{DR1}, \dots, |P_{[0 \text{ to } M_m-1]}\rangle_{DR_m}\}$ each of size $w = M_k \times \log_2|\Sigma|$ to store search pattern $P_k \in P = \{P_1, \dots, P_k, \dots, P_m\}$, and set of ancillary qubit designated to number of patterns $\{|q\rangle_{Q1}, \dots, |q\rangle_{Q_m}\}$
- Result : Outputs all t_k exact occurrence ($1 \leq t_k \leq N$) of each pattern $P_k \in P$ in parallel using c^{th} quantum core $QCore_c$ accessing T on shared QMEM, as index $|T_i\rangle_{QAk}$ s. t. $|T_{[i \text{ to } i+M_k-1]}\rangle_{QDk} == |P_{[0 \text{ to } M_k-1]}\rangle_{DRk}$
- 1: Procedure EnQPBEA-MPM
 - 2: Prepare registers as $|zeroes_n\rangle$ in $|T_n\rangle_{QAk}$, $|zeroes_{[w]}\rangle$ in $|T_{[w]}\rangle_{QDk}$, $|1\rangle$ in $|q\rangle_{Qk}$ and $|P_{[0 \text{ to } M_k-1]}\rangle_{DRk}$
 - 3: For each pattern $P_k \in P$ to be processed separately on c^{th} quantum core $QCore_c$
 - 4: Initialize quantum state in registers as $|\psi_n\rangle_k$ in $|T_i\rangle_{QAk}$, $|same_{[w]}\rangle$ in $|T_{[w]}\rangle_{QDk}$ & $|q\rangle_{Qk}$ as $|-\rangle$
 - 5: For all $|T_i\rangle_{QAk}$ in their separate uniform quantum superposition state $|\psi_n\rangle_k$
 - 6: Load data at $|T_{[i]}\rangle_{QDk}$ as per entangled $|T_i\rangle_{QAk}$ by applying QMEM Transformation as
 - 7: $U_{\text{Load}}(|T_i\rangle_{QAk} \otimes |T_{[w]}\rangle_{QDk}) = U_{\text{Load}}(|T_i\rangle_{QAk} \otimes |T_{[w \oplus i]}\rangle_{QDk}) = |T_i\rangle_{QAk} \otimes |T_{[i]}\rangle_{QDk}$
 - 8: Repeat GSO for $O(\sqrt{N}/t_k)$ times in uniform superposition $|\psi_n\rangle_k$, with QEM Operation which is implicitly applied through $U_{k\text{Comp}}$ for exact matching of $M_k \times \log_2|\Sigma|$ qubits size as -
 - 9:
$$U_{k\text{Comp}} \cdot f(|T_i\rangle_{QAk}) = \begin{cases} 0, & \text{if } |T_{[i \text{ to } i+M_k-1]}\rangle_{QDk} \neq |P_{[0 \text{ to } M_k-1]}\rangle_{DRk} \\ 1, & \text{if } |T_{[i \text{ to } i+M_k-1]}\rangle_{QDk} = |P_{[0 \text{ to } M_k-1]}\rangle_{DRk} \end{cases}$$

GSO Operation $\leftarrow (D \leftarrow U_{\text{Diff}}(O \leftarrow (U_{\text{Mark}}(U_{\text{Comp}}))))$
 - 10: End of GSO Repeat
 - 11: Measure the final state to get the desired index $|T_i\rangle_{QAk}$ as high probable solution
 - 12: Verify pattern P_k at $|T_i\rangle_{QAk}$ on c^{th} core $QCore_c$ as $|T_{[i \text{ to } i+M_k-1]}\rangle_{QDk} == |P_{[0 \text{ to } M_k-1]}\rangle_{DRk}$
 - 13: End of Inner For
 - 14: End of Outer For
 - 15: End Procedure

in a coherent superposition of text addresses. Once these substrings are available in parallel, EnQPBEA applies the GSO operator, separately on $QCore_c$ to ensure an exact match of each P_k with QEM circuit realized using $U_{k\text{Comp}}$. The Boolean oracle circuit succeeds by flipping target qubit of Fig. 3 to report exactness. When c^{th} core $QCore_c$ identifies exact match in superposition, the amplification operator $U_{\text{Diff}}(U_{\text{Mark}})$ is then applied to increase the probability amplitude of identified indices $|T_i\rangle_{QAk}$. The GSO operator repeats for $O(\sqrt{N})$ time and then $QCore_c$ applies the measurement to obtain search index $|T_i\rangle_{QAk}$ with high probability.

The quantum state gets collapsed after each measurement, so its repetition ensures to report all t_k index locations of $P_k \in P$ which are identified by c^{th} quantum core $QCore_c$. Each pattern occurrence is verified by same core as $|T_{[i \text{ to } i+M_k-1]}\rangle_{QDk} == |P_{[0 \text{ to } M_k-1]}\rangle_{DRk}$. The pattern matching method of EnQPBEA-MPM is illustrated in Fig. 4. However, the steps are listed in the proposed algorithm, and the equivalent quantum circuit executing search oracles in parallel is shown in Fig. 5. In reference to Table 4 discussion, we state, that each core realizes $O(\sqrt{N}/t_k)$ iterations of GSO in parallel, and therefore, results in all desired pattern occurrence t_k on behalf of pattern P_k . However, we require

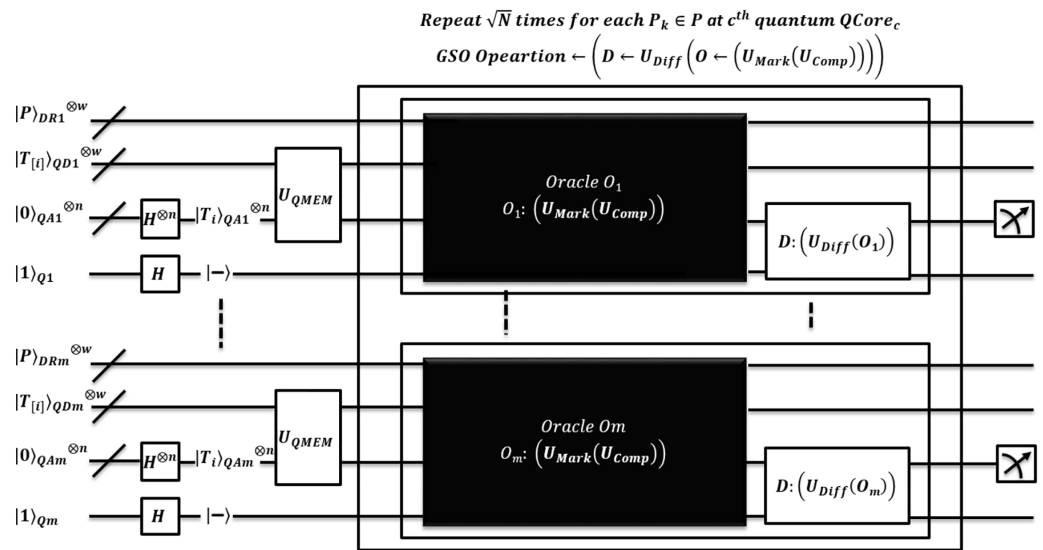


Figure 5 Quantum circuit equivalent to search mechanism of EnQPBEA-MPM algorithm.

Full-size DOI: 10.7717/peerj-cs.957/fig-5

$O(\sqrt{Nt_k})$ queries to report all t_k marked occurrences, and hence the pattern matching time is bounded to $O(\sqrt{Nt_k} \log_2 N)$ with negligible logarithmic factor. We clarify that EnQPBEA repeats GSO operation in parallel for t_k times on each core $QCore_c$ to search all t_k indexes. So, we consider $t = t_k = \max(t_1, \dots, t_k, \dots, t_m)$ as based on longest core processing to find maximum pattern occurrences. Therefore, the search complexity of parallel executions of EnQPBEA using QPU with C cores is $O((m/C)(\sqrt{Nt} \log_2 N))$ time. In support of complexities, a correctness proof of EnQPBEA-MPM with quantum operations is specified in [Appendix C](#). For mathematical proof, we define certain Lemma 1 as partial required proof, and based on that, we conclude the computational complexity and achieved speedup through the resulting proof of Theorem 1.

Lemma 1: A QPU having C quantum cores ($1 \leq c \leq C$) can access the text T of size N on shared QMEM. It loads all text substring equal to pattern length P_k as $M_k * \log_2 |\Sigma|$ qubits in superposition by using $QCore_c$ in parallel. Time needed for such parallel loading operations ranges between $O((m/C)(M \log_2 N))$ and $O((m/C)(MN \log_2 N))$.

Proof (Lemma 1): About earlier discussions of effective processing framework and [Table 4](#), we use to prove this lemma. The $|T_{2^n \times w}\rangle_{QMEM}$ as shared among C cores of QPU, makes sure that all $|T_i\rangle_{QAk}$ addresses are available in parallel on each $QCore_c$ & QMEM transformation loads $M_k * \log_2 |\Sigma|$ qubits in entangled register $|T_{[w]}\rangle_{QDk}$. The entire memory access is available in constant time on each individual core, however, by considering M as $M = \max(M_1, \dots, M_k, \dots, M_m)$ the memory circuit needs $O(M \log_2 N)$ steps. So, the parallel time of QMEM access using QPU with C quantum cores is $O((m/C)(M \log_2 N))$. As we know, that the quantum state is collapsed after each measurement, so to report all t_k index of P_k identified by c^{th} quantum core $QCore_c$, we need this access several times. By assuming $t = t_k = \max(t_1, \dots, t_k, \dots, t_m)$ at any $QCore_c$ for

QMEM transformation, and at worst, if number of identified patterns are $t = N$ then each time, all parallel substring load will take $O((m/C)(MN\log_2 N))$ time. We discussed earlier, that both these factors M and (m/C) are negligible due to parallel load and parallel processing by achieving exponential speedup.

Theorem 1: Given text database T of size N and the multiple patterns set $P = \{P_1, \dots, P_k, \dots, P_m\}$ with each pattern P_k of length $M_k (1 \leq k \leq m)$. Algorithm EnQPBEA-MPM uses QPU having C quantum cores ($1 \leq c \leq C$) to access the text T on shared QMEM. A c^{th} core is used to search for the all t_k exact occurrence of a pattern P_k indexed at $|T_i\rangle_{QAK}$, that is $|T_{[i \text{ to } i+M_k-1]}\rangle_{QDK} = |P_{[0 \text{ to } M_k-1]}\rangle_{DRK}$. Based on longest core processing to find pattern occurrences $t = \max(t_1, \dots, t_k, \dots, t_m)$, the search time complexity of EnQPBEA-MPM is $O((m/C)(\sqrt{N}t\log_2 N))$ in the best case and $O((m/C)(N\log_2 N))$ for the worst case.

Proof (Theorem 1): This proof relies on Lemma 1 and other statements which are justified earlier. Proof of Lemma 1 states that, for $t = 1$ or t_{few} (t_{few} denotes few pattern occurrences ($t_{\text{few}} \ll N$)) and $t = N$, all substring load transformation is possible in $O(\log_2 N)$ and $O(N\log_2 N)$ time. Now EnQPBEA-MPM algorithm realizes such parallelism using QPU with C quantum cores and each core access text T on shared QMEM. For each pattern $P_k \in P$ of length $M_k (1 \leq k \leq m)$, this algorithm identifies the target indices based on the QEM circuit under superposition of N sized text. Further, the simultaneous iterations of GSO finds all t_k solutions of P_k using c^{th} quantum core $QCore_c$ in $O((m/C)(\sqrt{N/t_k}))$ queries.

Indeed, quantum state is collapsed while measured, so, EnQPBEA repeats GSO followed by measurement on $QCore_c$ to report all t_k occurrence of P_k in $O((m/C)(\sqrt{N/t_k}))$ queries. Now, based on longest core processing, consider $t = t_k = \max(t_1, \dots, t_k, \dots, t_m)$. So, using QPU with C cores and for $t = 1$ or t_{few} (t_{few} denotes few pattern occurrences ($t_{\text{few}} \ll N$)), the best case time complexity of EnQPBEA-MPM is $O((m/C)(\sqrt{N}t\log_2 N))$ and this finds all patterns in parallel. However, when $t = N$ (all are search solutions), the worst-case time complexity is $O((m/C)(N\log_2 N))$. A multiplicative factor ($\log_2 N$) is considered negligible with n qubits, surprisingly small, to expand the original search space. However, this factor cannot be ignored when the number of qubits n is usually large to expand the original text space (Lomont, 2003). And the multiplicative constant (m/C) with a small arbitrary constant value of m and constant value of C is found negligible. However, for the comparatively large value of $m \gg C$, a factor m/C cannot be ignored in time complexities. Therefore, quantum search is preferred effectively for finding few occurrences. Instead, for biological text, $t = N$ is rare and hence ignored while stating the generalized complexity. We know that algorithm design is based on GSO, so, results are obtained with at least probability as $Pr[\text{EnQPBEA running at } QCore_c \text{ measures } |T_i\rangle_{QAK} \text{ in each iteration}] \geq t_k/N$.

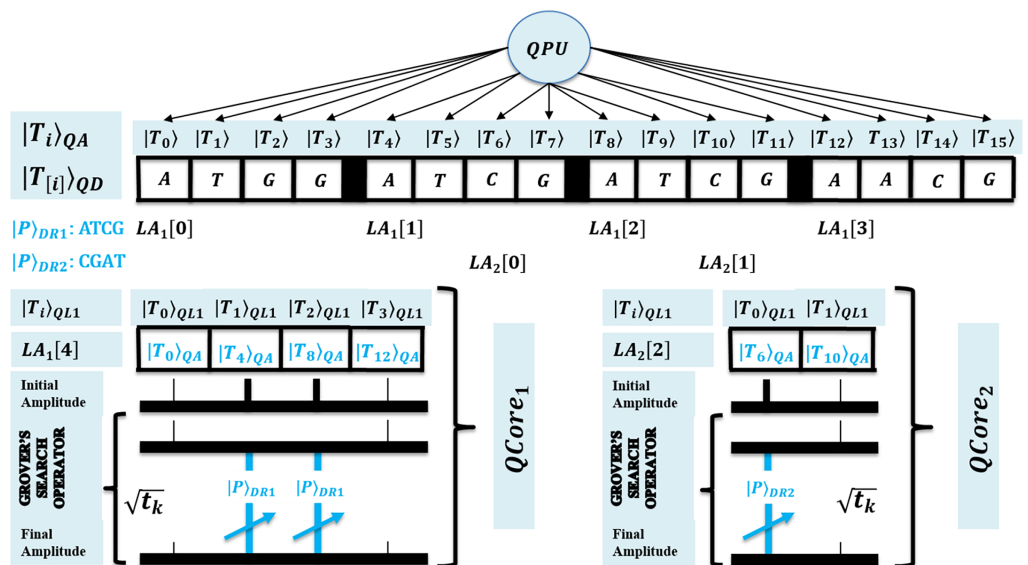


Figure 6 Quantum-based illustration of the EnQBCEA-MPM algorithm.

Full-size DOI: 10.7717/peerj-cs.957/fig-6

Proposed method 2: enhanced quantum-based combined exact algorithm for multiple pattern matching EnQBCEA-MPM

The algorithm EnQBCEA-MPM is an enhanced version of the existing benchmark method QBCE. So, we formalize this multiple pattern algorithm with the possible speedup. The pattern matching method is illustrated in Fig. 6. Each pattern $P_k \in P$ is individually processed using QPU with C cores; however, the c^{th} core $QCore_c$ ($1 \leq c \leq C$) processes the text T of size N over shared QMEM for (m/C) patterns either for filtering or searching. In this method, each core $QCore_c$ transforms the original N sized text into reduced search space t_k (corresponding to P_k), so-called filtered indices, and then performs exact searching of all t_k occurrence of each P_k in overlapping of time evolution. To transform the text into reduced search space, we use an existing method of quantum-approximate filtering (QAF). This method is based on the hamming distance (HD) to check for the possible errors between pattern and text substring (to filter index) and ensures its correctness when the hamming distance (HD) \leq threshold (pre-computed). Such filtering outcomes are based on approximations, thus, we verify the filtered indices for a pattern match using the exactness. An additional time of QAF filtering is included in the complexity of this algorithm; however, this allows searching of patterns in an optimized way by achieving speedup. Our EnQBCEA design executes exact search oracles in parallel with the negligible time factor, and this also removes the existing iterative overhead (text filtering and pattern searching) of the QAMP algorithm. We expect the pattern matching results as effective for the biological sequencing because of overlapped quick search time to find the exact matches over the filtered text indices.

Initially, we redefine QAF (Aborot, 2017) to execute for each $QCore_c$ while accessing text T on shared QMEM for text filtering. The procedure QAF is redesigned here by using QMEM transformation. This prepares the pattern in register $|P\rangle_{DR}$ and the start locations

Procedure: $QAF(|T_n\rangle_{QA}, |P\rangle_{DR}, LA[\dots])$.

Input : Text address register $|T_n\rangle_{QA}$, auxiliary register of same size with additional qubit $|T_{n+1}\rangle_{AX}$, the implicit data register $|P_{[0 \text{ to } M-1]}\rangle_{DR}$, $SL[M]$ classical array that keeps distinct symbol location within pattern as $|i_j\rangle$, access to location array $LA[\dots]$ to classically store filtered text indices.

Output : Stores all filtered text indices as possible start of pattern in location array $LA[\dots]$

- 1: Begin Procedure
- 2: Prepare P in $|P_{[0 \text{ to } M-1]}\rangle_{DR}$, and store $|i_j\rangle$ in $SL[M]$ as preprocessed start locations of distinct symbol of $|P\rangle_{DR}$
- 3: Prepare registers as $|zeroes_n\rangle$ in $|T_n\rangle_{QA}$, $|zeroes_{[w]}\rangle$ in $|T_{[w]}\rangle_{QD}$, $|zeroes_{n+1}\rangle$ in $|T_{n+1}\rangle_{AX}$
- 4: Initialize State as $|\psi_n\rangle$ in $|T_i\rangle_{QA}$, $|same_{[w]}\rangle$ in $|T_{[w]}\rangle_{QD}$ & entangle the register $|T_{n+1}\rangle_{AX}$
- 5: Load data at $|T_{[i]}\rangle_{QD}$ as per entangled $|T_i\rangle_{QA}$ by applying QMEM Transformation as
- 6: $U_{Load}(|T_i\rangle_{QA} \otimes |T_{[w]}\rangle_{QD}) = U_{Load}(|T_i\rangle_{QA} \otimes |T_{[w \oplus i]}\rangle_{QD}) = |T_i\rangle_{QA} \otimes |T_{[i]}\rangle_{QD}$
- 7: For each $|T_i\rangle_{QA}$ remains in uniform quantum superposition state $|\psi_n\rangle$ do
- 8: Mark distinct symbol of pattern by unitary U_{SLoc} as $|T_{i_j}\rangle_{AX}$ corresponding to $|T_i\rangle_{QA}$
- 9: Mark possible start location of pattern by U_{PLoc} as $|T_i - T_{i_j}\rangle_{AX}$ on behalf of $|T_i\rangle_{QA}$
- 10: Apply HD at $|T_i - T_{i_j}\rangle_{AX}$ to check for distance between text and pattern, such that, $HD \leq \text{threshold}$
- 11: Apply Hadamard at $|T_i\rangle_{QA}$ to merge amplitudes of entangled indices of $|T_i - T_{i_j}\rangle_{AX}$
- 12: Measure the auxiliary register $|T_i - T_{i_j}\rangle_{AX}$ and store the identified index as $|T_i\rangle$ in $LA[\dots]$
- 13: End of For
- 14: End Procedure

of distinct symbols of the pattern are store in array $SL[M]$. Now, initializes QMEM registers $|T_n\rangle_{QA}$ and $|T_{[w]}\rangle_{QD}$ in the zero state along with auxiliary register $|T_{n+1}\rangle_{AX}$ measured for the filtered index as possible start locations of the pattern. The superposition of text created in $|T_i\rangle_{QA}$ and $|T_{n+1}\rangle_{AX}$ is made entangled with addresses. Under memory superposition of $|T_i\rangle_{QA}$, QAF marks the distinct symbols of the pattern at $|T_{i_j}\rangle_{AX}$ by unitary U_{SLoc} . And then, the possible start location of the patterns are marked as $|T_i - T_{i_j}\rangle_{AX}$ by U_{PLoc} . A Hamming distance (HD) is applied at $|T_i - T_{i_j}\rangle_{AX}$ to check for threshold, further, Hadamard is applied at $|T_i\rangle_{QA}$ to merge probability amplitudes of entangled indices of $|T_i - T_{i_j}\rangle_{AX}$. Finally, measure auxiliary register $|T_i - T_{i_j}\rangle_{AX}$ to identify filtered indices $|T_i\rangle$ which are then stored in the referenced location array $LA[\dots]$. As measurement destroys quantum state, so in each call at c^{th} quantum core $QCore_c$ on behalf of $P_k \in P$, the QAF needs its execution several times to filter all t_k indices location and then to store within the location array $LA_k[t_k]$.

Algorithm EnQBCEA-MPM needs following preparation such as – each pattern $P_k \in P$ is assumed with individual size $w = M_k * \log_2|\Sigma|$ qubits, and it is stored in $|P_{[0 \text{ to } M_k-1]}\rangle_{DRk}$ as in separate data register. At first, procedure $QAF(|T_n\rangle_{QAk}, |P_k\rangle_{DRk}, LA_k)$ is called for each pattern P_k on each core to store the filtering results at individual location array $LA_k[t_k]$. Each $LA_k[\dots]$ contained with $t_k \leq N$ filtered text indices; therefore, the algorithm needs location register $|T_{tq}\rangle_{QLk}$ each of size $\log_2 t_k = tq$ qubits to access $LA_k[t_k]$ by using c^{th} core $QCore_c$.

Proposed Algorithm 2: EnQBCEA-MPM.

- Data : Text T stored on $|T_{2^n \times w}\rangle_{QM\text{EM}}$ which is accessed by quantum registers $\{|T_n\rangle_{QA1}, \dots, |T_n\rangle_{QAm}\}$ and $\{|T_w\rangle_{QD1}, \dots, |T_w\rangle_{QDm}\}$, the implicit data registers $\{|P_{[0 \text{ to } M_1-1]}\rangle_{DR1}, \dots, |P_{[0 \text{ to } M_m-1]}\rangle_{DRm}\}$ each of size $w = M_k \times \log_2|\Sigma|$ to store search pattern $P_k \in P = \{P_1, \dots, P_k, \dots, P_m\}$, separate location arrays $\{LA_1[\dots], \dots, LA_m[\dots]\}$ to classically store $\{t_1, \dots, t_m\}$ filtered text indices corresponding to each P_k , location registers to access filtered indices for each pattern as $\{|T_{tq}\rangle_{QL1}, \dots, |T_{tq}\rangle_{QLm}\}$ each with size $\log_2 t_k = tq$ qubits, & set of ancillary qubits designated to no. of pattern $\{|q\rangle_{Q1}, \dots, |q\rangle_{Qm}\}$
- Result : Outputs all t_k exact occurrence ($1 \leq t_k' \leq t_k$) of each pattern $P_k \in P$ in parallel, using c^{th} quantum core $Q\text{Core}_c$ accessing filtered location array $LA_k[t_k]$ which is explored on $QM\text{EM}$, as searched index $|T_{iLk}\rangle_{QAk}$ s.t. $|T_{[iLk \text{ to } iLk + M_k - 1]}\rangle_{QDk} == |P_{[0 \text{ to } M_k - 1]}\rangle_{DRk}$
- 1: Procedure EnQBCEA-MPM
 - 2: For each pattern $P_k \in P$ to be processed separately on c^{th} quantum core $Q\text{Core}_c$
 - 3: Call $QAF(|T_n\rangle_{QAk}, |P_k\rangle_{DRk}, LA_k)$;
 - 4: End of For
 - 5: Prepare registers as $|zeroes_{tq}\rangle$ in $|T_{tq}\rangle_{QLk}$, $|zeroes_n\rangle$ in $|T_n\rangle_{QAk}$, $|zeroes_w\rangle$ in $|T_w\rangle_{QDk}$, $|1\rangle$ in $|q\rangle_{Qk}$ and $|P_{[0 \text{ to } M_k - 1]}\rangle_{DRk}$
 - 6: For each pattern $P_k \in P$ to be processed separately on c^{th} quantum core $Q\text{Core}_c$
 - 7: Initialize quantum state for accessing $LA_k[t_k]$ in register as $|\psi_{tq}\rangle_k$ in $|T_i\rangle_{QLk}$, $|T_{[i]}\rangle_{QLk}$ in $|T_i\rangle_{QAk}$, $|same_w\rangle$ in $|T_w\rangle_{QDk}$, $|q\rangle_{Qk}$ as $|-\rangle$
 - 8: For all $|T_i\rangle_{QLk}$ in their separate uniform quantum superposition state $|\psi_{tq}\rangle_k$
 - 9: Apply the unitary $U_{k\text{GetL}}$ to get n -qubits actual index as $|T_{[i]}\rangle_{QLk} = iLk$ i.e. the memory content of $LA_k[t_k]$ through $|T_i\rangle_{QLk}$, and then store k^{th} address in corresponding register $|T_{iLk}\rangle_{QAk}$
 - 10: $U_{k\text{GetL}}: f(|T_i\rangle_{QLk}) = |T_i\rangle_{QLk}|T_{[i]}\rangle_{QLk}\rangle_{QAk} \rightarrow |T_i\rangle_{QLk}|T_{iLk}\rangle_{QAk}$
 - 11: Load data at $|T_{[iLk]}\rangle_{QDk}$ as per addresses $|T_{iLk}\rangle_{QAk}$ by applying $QM\text{EM}$ Transformation as
 - 12: $U_{\text{Load}}(|T_{iLk}\rangle_{QA} \otimes |T_w\rangle_{QD}) = U_{\text{Load}}(|T_{iLk}\rangle_{QAk} \otimes |T_{[w \oplus i]}\rangle_{QDk}) = |T_{iLk}\rangle_{QAk} \otimes |T_{[iLk]}\rangle_{QDk}$
 - 13: Repeat GSO for $O(\sqrt{t_k/t_k'})$ times in uniform superposition $|\psi_{tq}\rangle_k$, with QEM Operation which is implicitly applied through $U_{k\text{Comp}}$ for exact matching of $M_k \times \log_2|\Sigma|$ qubits size as -
 - 14: $U_{\text{Comp}}: f(|T_{iLk}\rangle_{QAk}) = \begin{cases} 0, & \text{if } |T_{[iLk \text{ to } iLk + M_k - 1]}\rangle_{QDk} \neq |P_{[0 \text{ to } M_k - 1]}\rangle_{DRk} \\ 1, & \text{if } |T_{[iLk \text{ to } iLk + M_k - 1]}\rangle_{QDk} = |P_{[0 \text{ to } M_k - 1]}\rangle_{DRk} \end{cases}$
 - 15: GSO Operation $\leftarrow (D \leftarrow U_{\text{Diff}}(O \leftarrow (U_{\text{Mark}}(U_{\text{Comp}}))))$
 - 16: End of GSO Repeat
 - 17: Measure the final state to get the desired index $|T_{iLk}\rangle_{QAk}$ as high probable solution
 - 18: Verify pattern P_k at $|T_{iLk}\rangle_{QAk}$ on c^{th} core $Q\text{Core}_c$ as $|T_{[iLk \text{ to } iLk + M_k - 1]}\rangle_{QDk} == |P_{[0 \text{ to } M_k - 1]}\rangle_{DRk}$
 - 19: End of Inner For
 - 20: End of Outer For
 - 21: **End Procedure**

The algorithm EnQBCEA proceeds to search for each pattern by running all cores in parallel. An equivalent quantum circuit executing search oracles in parallel is shown in Fig. 7. So, each core $Q\text{Core}_c$ explores filtered indices of $LA_k[t_k]$ in superposition over $QM\text{EM}$. We expect that the reduced search space of size $t_k \ll N$ is small than that of original text T of size N . Algorithm prepares registers in $|zero\rangle$ states, and initializes superposition of filtered indices for each $LA_k[t_k]$ as $|\psi_{tq}\rangle_k$ by using $|T_i\rangle_{QLk}$ ($i \in \{0, 1\}^{tq}$) of $Q\text{Core}_c$. Now, for each $|T_i\rangle_{QLk}$ under the quantum superposition $|\psi_{tq}\rangle_k$ we apply $U_{k\text{GetL}}$ to obtain n - qubits original filtered index as $|T_{[i]}\rangle_{QLk} = iLk$ i.e. $[i]^{\text{th}}$ memory content of

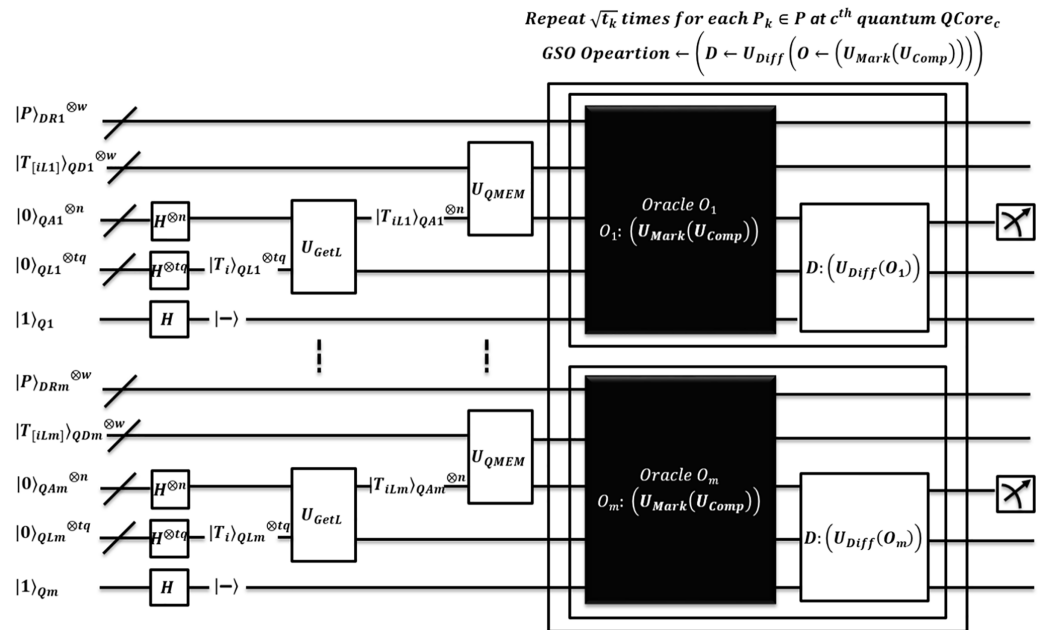


Figure 7 Quantum circuit equivalent to searching logic of the EnQBCEA-MPM algorithm.

Full-size DOI: 10.7717/peerj-cs.957/fig-7

$LA_k[t_k]$ through $|T_i\rangle_{QLk}$. This transformation helps address register $|T_{iLk}\rangle_{QAk}$ to access actual indices, so the search can perform over original text.

Now, the original text is available in QMEM superposition and shared among all quantum cores. Therefore, text T realized on $|T_{2^n \times w}\rangle_{QMEM}$ is accessed in a superposition of addresses by $QCore_c$ by address register $|T_{iLk}\rangle_{QAk}$ ($iLk \in \{0, 1\}^n$). All the text substrings, each of length $M_k * \log_2|\Sigma|$ are loaded in entangled register $|T_{iLk}\rangle_{QDk}$ by applying QMEM transformation. A unitary U_{Load} makes sure such loading is in a coherent superposition of text addresses. Once substrings are available in parallel, EnQBCEA applies GSO, by $QCore_c$ to find an exact match of each P_k with QEM circuit realized using the unitary operator U_{Comp} . The processing of GSO is the same as per earlier discussion of EnQPBEA and Table 4. Instead, each core realizes $O(\sqrt{t_k/t_k'})$ iterations of GSO in parallel, however, after $O(\sqrt{t_k})$ repetition $QCore_c$ applies measurement to obtain index $|T_{iLk}\rangle_{QAk}$ with high probability. As measurement collapses quantum state, so, each $QCore_c$ requires $O(\sqrt{t_k t_k'})$ queries to report all $t_k' \leq t_k$ marked occurrences of P_k in T . In addition, EnQBCEA-MPM allows c^{th} core $QCore_c$ to verify pattern match at $|T_{iLk}\rangle_{QAk}$ as $|T_{[iLk \text{ to } iLk+M_k-1]}\rangle_{QDk} == |P_{[0 \text{ to } M_k-1]}\rangle_{DRk}$. A correctness proof of EnQBCEA-MPM is included in Appendix D and complexity is proved in Theorem 2.

Lemma 2: A QPU having C quantum cores ($1 \leq c \leq C$) can access the text T of size N on shared QMEM. A c^{th} core filters t_k indices $|T_i\rangle_{QAk}$ in parallel to identify the possible start locations of pattern P and to store such original filtered indices in $LA_k[t_k]$. Time needed for executing quantum approximate filtering (QAF) in parallel is $O((m/C)(t \log_2 N))$.

Proof (Lemma 2): In support of the earlier discussions and using the reference to [Aborot \(2017\)](#) and [Soni & Rasool \(2021\)](#), we used to prove this lemma. Procedure QAF is executed in parallel for each pattern $P_k \in P$ on c^{th} quantum core $QCore_c$ sharing the QMEM. Quantum circuit included in [Aborot \(2017\)](#) and [Soni & Rasool \(2021\)](#) will runs separately on $QCore_c$ and performs equivalent quantum operations as U_{SLoc} , U_{PLoc} , HD followed by the Hadamard on $|T_i\rangle_{QAk}$ to merge probability amplitudes of entangled indices of $|T_i - T_j\rangle_{AX}$. Now auxiliary register measures filtered indices $|T_i\rangle$ to store in $LA[\dots]$. All such operations are bounded by $O(\log_2 N)$ time. However, measurement destroys quantum state, so in each call at c^{th} quantum core $QCore_c$ on behalf of $P_k \in P$, the QAF needs its repeated executions to filter all t_k indices and to store them in location array $LA_k[t_k]$. Therefore, based on longest core processing to filter maximum pattern locations, we assume $t = t_k = \max(t_1, \dots, t_k, \dots, t_m)$ at any $QCore_c$. The time required for such filtering in parallel is $O((m/C)(t \log_2 N))$. The multiplicative factors can be ignored due to parallel processing – quantum circuit operations.

Theorem 2: Given text database T of size N and the multiple pattern set $P = \{P_1, \dots, P_k, \dots, P_m\}$ with each pattern P_k of length $M_k (1 \leq k \leq m)$. Algorithm EnQBCEA-MPM uses QPU having C quantum cores ($1 \leq c \leq C$) to access the text T on shared QMEM. The c^{th} core runs QAF to store all t_k filtered indices of a pattern P_k in $LA_k[t_k]$. The indices of $LA_k[t_k]$ are used by c^{th} core to search for all $t_{k'}$ exact occurrence of patterns indexed at $|T_{iLk}\rangle_{QAk}$, that is $|T_{[iLk \text{ to } iLk+M_k-1]}\rangle_{QDk} == |P_{[0 \text{ to } M_k-1]}\rangle_{DRk}$. Based on maximum filtered indices $t = \max(t_1, \dots, t_k, \dots, t_m)$ in $LA_k[t]$ and longest core processing to find pattern occurrences $t' = \max(t_{1'}, \dots, t_{k'}, \dots, t_{m'})$, the search time complexity of EnQBCEA-MPM algorithm is $O((m/C)(\sqrt{tt'} \log_2 t))$ in the best case and $O((m/C)(t \log_2 t))$ for the worst case.

Proof (Theorem 2): The proof of this theorem is based on Lemma 2 and other statements which are justified earlier. Our algorithm EnQBCEA-MPM performs a search on filtering outcomes that are stored in parallel by executing the QAF on separate quantum cores. It is assured that EnQBCEA performs the search on reduced size text database T , each of size t_k . Thus, this increases the success probability for identifying the search results. Lemma 2 states, that to store all t_k filtered indices in $LA_k[t_k]$ we need $O((m/C)(t \log_2 N))$ time. Each core $QCore_c \in QPU$ utilizes the processing advantage of QMEM in both filtering and searching. Algorithm EnQBCEA-MPM accesses $LA_k[t_k]$ on each $QCore_c$ to obtain the original filtered text indices by applying unitary $U_{k\text{GetL}}$. It takes $O(1)$ time for realizing such transformation under the superposition.

The original text is available in QMEM superposition and shared among all quantum cores. Thus, each $QCore_c$ applies QMEM transformation to load all substrings in parallel, such that, each pattern $P_k \in P$ of length $M_k (1 \leq k \leq m)$ verifies for exactness over filtered index approximations. Now, based on the QEM circuit applied under the superposition of t_k sized text T , the indices are identified for an exact match. Further, parallel iterations of GSO finds all $t_{k'}$ ($t_{k'} \leq t_k$) solutions of P_k using c^{th} core $QCore_c$ in

$O\left(\frac{m}{C}\left(\sqrt{\frac{t_k}{t_{k'}}}\right)\right)$ queries. Indeed, the quantum state collapsed while measured; therefore, EnQBCEA repeats GSO operation followed by measurement, on each quantum core $QCore_c$ to report all $t_{k'}$ exact occurrences of the pattern P_k in resulting $O\left(\frac{m}{C}\left(\sqrt{t_k t_{k'}}\right)\right)$ queries and thus $O\left(\frac{m}{C}\left(\sqrt{t_k t_{k'}} \log_2 t_k\right)\right)$ time.

To conclude the complexity, we are considering the maximum reduced size of any filtered location array $LA_k[t_k]$ as $t = t_k = \max(t_1, \dots, t_k, \dots, t_m)$, and the longest core processing to find maximum pattern occurrences $t' = t_{k'} = \max(t_{1'}, \dots, t_{k'}, \dots, t_{m'})$. So, using QPU with C cores and for $t' = 1$ or t_{few} (t_{few} denotes few pattern occurrences ($t_{\text{few}} \ll t$)), the best case time complexity of EnQBCEA-MPM is $O\left(\frac{m}{C}\left(\sqrt{t t'} \log_2 t\right)\right)$ and this finds all patterns in parallel. However, when $t' = t$ the worst-case complexity is still bounded to $O\left(\frac{m}{C}\left(t \log_2 t\right)\right)$. A multiplicative factor ($\log_2 t$) is considered negligible as due to less qubits ($tq \ll n$) needed to expand the reduced search space. However, this factor cannot be ignored when the number of qubits tq is sufficiently large to expand the filtered space (Lomont, 2003; Soni & Rasool, 2021). And the multiplicative constant (m/C) with a small arbitrary constant value of m and constant value of C is found negligible. However, for the comparatively large value of $m \gg C$, a factor m/C cannot be ignored in time complexities. Therefore, quantum search is preferred effectively for few occurrences. Instead, for biological text, $t' = t$ is rare and hence ignored while stating a generalized complexity. We also suggest that algorithm design based on the functionality of GSO, enhances the results with probability

$$Pr\left[\text{EnQBCEA running at } QCore_c \text{ measures } |T_{iLk}\rangle_{QAK} \text{ in each iteration}\right] \geq t_{k'}/t_k.$$

THEORETICAL RESULTS AND COMPLEXITIES ANALYSIS

The presented algorithms EnQPBEA-MPM and EnQBCEA-MPM are hereby observed with summarized facts of several complexities analysis. This section incorporates the design methods by mainly focusing on actual qubits requirement. For dealing with number of unknown search solutions, the analysis of quantum counting algorithms is included. An idea to simulate QMEM is also discussed here with the realization of quantum effective processing framework.

Summarized complexities analysis and mathematical proved results

We summarize our proven results to compare with the related work. The significant findings were noted herein dedicated tables to emphasize our analytical interpretation. In this section, we present the concluded complexities of our algorithms using Tables 5 and 6 is referred for discussing the design methods with qubits requirement and success probability.

Analysis of proposed algorithms based on several quantum complexities:

- The resulting complexities of algorithms have been proved earlier and summarized in Table 5. In reference to Tables 1–3, we discuss comparative factors of our work.
- Our algorithms obtain speedup with effective quantum processing while comparing with the classical searching time of $O(mN)$ (discussed in the introduction). The classical

Table 5 Summarized quantum complexities of the proposed algorithms.

Quantum algorithm	Pre-processing complexity	Proposed quantum pattern searching time complexity				Storage complexity (qubits estimation)
		Query	Best time	Worst time	Generalized	
EnQPBEA-MPM	No Text Filtering	$O\left(\frac{(m/C)}{\sqrt{Nt}}\right)$	$O\left(\frac{(m/C) \times}{(\sqrt{Nt} \log_2 N)}\right)$	$O\left(\frac{(m/C) \times}{(N \log_2 N)}\right)$	$O((m/C)\sqrt{N})$	$O\left(\frac{(m/C) \times}{(n + M \log_2 \Sigma)}\right)$
EnQBCEA-MPM	$O\left(\frac{(m/C) \times}{(t \log_2 N)}\right)$	$O\left(\frac{(m/C)}{\sqrt{tt'}}\right)$	$O\left(\frac{(m/C) \times}{(\sqrt{tt'} \log_2 t)}\right)$	$O\left(\frac{(m/C) \times}{(t \log_2 t)}\right)$	$O((m/C)\sqrt{t})$	$O\left(\frac{(m/C) \times}{(n + M \log_2 \Sigma + \log_2 t)}\right)$

Table 6 Framework and design of proposed algorithms with qubits requirement and success probability.

Quantum algorithm	Algorithm framework	Algorithm design	Quantum registers requirement	Actual qubits requirement	Success probability
EnQPBEA-MPM	QMEM, QEM, GSO	QPBE Algorithm, Multiple Search Oracle, QPU (C-Quantum Cores)	$ T_n\rangle_{QA} : m/C,$ $ T_{ w }\rangle_{QD} : m/C, P_M\rangle_{DR} : m/C, q\rangle : m/C$	$(m/C) \times (n + (2(M \log_2 \Sigma) + 1))$	$Pr(QCore_k) \geq t_k/N$
EnQBCEA-MPM	QMEM, QEM, GSO	QBCE Algorithm, Multiple Search Oracle, QPU (C-Quantum Cores)	$ T_n\rangle_{QA} : m/C,$ $ T_{n+1}\rangle_{AX} : m/C,$ $ T_{ w }\rangle_{QD} : m/C,$ $ T_{ q }\rangle_{QL} : m/C$ $ P_M\rangle_{DR} : m/C, q\rangle : m/C$	$(m/C) \times (2n + 2(M \log_2 \Sigma) + tq + 1)$	$Pr(QCore_k) \geq t_k/t_k$

worst-case time with characters comparison is $O(m(NM))$ instead, each core of QPU sharing QMEM does parallel match by U_{kComp} , and hence this makes our solutions $O((m/C)\sqrt{N})$ and $O((m/C)\sqrt{t})$ as efficient.

- We enhanced the QPBE and QBCE for multiple patterns under quantum architectural and implicit operational parallelism. Based on complexity analysis, our solutions are proved efficient to find an exact match while comparing with existing multiple pattern methods QEMP and QAMP as the factor m cannot be excluded from their complexities.
- Our algorithm designs execute exact search oracles in parallel using individual quantum core. The processing time for few pattern occurrences ($t_{few} \ll N$) is negligible, and we need less qubits to expand the filtered search space. A QPU runs C cores to search for m/C pattern in parallel, and each quantum core uses its own set of register. So multiplicative constant (m/C) with a small arbitrary constant value of m and constant value of C is found negligible. But, for comparatively large value of $m \gg C$, factor m/C cannot be ignored in time complexities.
- We included the storage complexity of our algorithms to estimate the qubits requirement. This complexity is based on the asymptotic estimation of qubits by excluding constants. Later, in Table 6, we specify actual qubits requirement with coefficients to check simulation feasibility of algorithms, as classical machine configuration is restricted to simulate large qubits.
- Quantum algorithms and their quantum circuits are proved equivalent for implementations. Therefore, the quantum query, time and storage complexities of

proposed algorithms justify their effectiveness. All the requisite and relevant discussions on behalf of Table 5 have been discussed earlier as per the contextual need.

Design methods used for quantum multiple pattern matching algorithms:

- Table 6 shows framework and design of algorithms. Used quantum registers are mentioned to check for proportional simulation feasibility of actual qubits requirement. Search success probability on any $QCore_c$, proved in theorems, is based on original and filtered text sizes.
- The quantum results may contain error while measured; therefore, GSO operation is used to amplify the probability amplitudes. Thus, we obtain the search results with a high probability. Therefore, we categorize our algorithms in BQP complexity class.
- The qubits are implicitly analyzed based on the quantum register requirement. For QPU with C cores based parallel processing, this (m/C) factor is there; however, these cores use their own set of quantum registers, so the factor is negligible, and time is reduced in parallelism.
- Classical machine configuration is restricted to simulate large qubits and affects simulation. Therefore, algorithms are implemented using hybrid simulation, such that each core can use the sufficient qubits with no excessive increase in qubits requirement of a quantum system.
- To save qubits requirement, EnQPBEA and EnQBCEA are simulated by using ANF based quantum operations, dedicated use of ancillary qubits, and utilizing QuEST specific unitary for efficient realization. The hybrid simulation results are noted later in the tables included in “Simulation Results and Discussion” section.

Exact and approximate quantum counting complexity analysis

Quantum counting (QC) is a quantum amplitude estimation method to handle the case of GSO overshooting as t number of search solutions are unknown in advance, so it leads to the unknown number of GSO iterations (Brassard et al., 2002; Nielsen & Chuang, 2010; Song, 2017). These authors (Boyer et al., 1998; Brassard et al., 2002; Lomont, 2003; Younes, 2008) suggested running the quantum counting algorithm initially and then proceeding with the actual number of GSO iterations. We obtained an accurate t value by implementing Exact-QC and the estimated t value through Approx.-QC methods. We provide the complexities analysis of both these cases in the subsection, and the resulting complexities are specified in Table 7.

Analysis of approximate and exact quantum counting (QC) algorithms:

- For EnQPBEA algorithm, QC is available with the $O(\sqrt{N})$ query and $O(\sqrt{N}\log_2 N)$ time. Approx.-QC algorithm can estimate the value of t with some relative error. In contrast, Exact-QC algorithm with $O(\sqrt{Nt})$ query and $O(\sqrt{Nt}\log_2 N)$ time can find the accurate value of t with the high probability (Boyer et al., 1998; Brassard et al., 2002; Lomont, 2003; Younes, 2008). Similarly the EnQBCEA algorithm, working on t filtered indices to find t' pattern occurrences, needs $O(\sqrt{t})$ query and $O(\sqrt{t}\log_2 t)$ time in

Table 7 Analysis of QC algorithm used to find approximate or exact value of t as number of search solutions.

Quantum counting	Algorithm framework	Analyzed complexities for EnQPBEA-MPM			Analyzed Complexities for EnQBCEA-MPM		
		Query	Time	Storage	Query	Time	Storage
Approx. - QC	QAE	$O\left(\frac{(m/C)}{\sqrt{N}}\right)$	$O\left(\frac{(m/C)\times}{(\sqrt{N}\log_2 N)}\right)$	$O\left(\frac{(m/C)\times}{(n+r)}\right)$, and ($r < n$)	$O\left(\frac{(m/C)}{\sqrt{t}}\right)$	$O\left(\frac{(m/C)\times}{(\sqrt{t}\log_2 t)}\right)$	$O\left(\frac{(m/C)\times}{(tq+r)}\right)$, and ($r < tq$)
Exact-QC	QAE	$O\left(\frac{(m/C)}{\sqrt{Nt}}\right)$	$O\left(\frac{(m/C)\times}{(\sqrt{Nt}\log_2 N)}\right)$	$O\left(\frac{(m/C)\times}{(n+r)}\right)$, and ($r = n$)	$O\left(\frac{(m/C)}{\sqrt{t'}}$	$O\left(\frac{(m/C)\times}{(\sqrt{t'}\log_2 t)}\right)$	$O\left(\frac{(m/C)\times}{(tq+r)}\right)$, and ($r = tq$)

Approx.-Q algorithm, and $O(\sqrt{tt'})$ query and $O(\sqrt{tt'}\log_2 t)$ time in Exact-QC algorithm (Brassard et al., 2002; Soni & Rasool, 2021). In Table 7, we have shown the complexities by including (m/C) factor because the quantum counting is needed to run on individual quantum core for each pattern separately.

- To measure the accurate value of t through Exact-QC we used to take the register with the precision qubits " r " $\approx (\log_2 N = n)$ qubits for EnQPBEA and " r " $\approx (\log_2 t = tq)$ qubits for EnQBCEA algorithm. Similarly, to measure the approximation of the value of t through Approx.-QC we need a register with precision qubits " r " $< \log_2 N$ qubits for EnQPBEA and " r " $< \log_2 t$ qubits for EnQBCEA algorithm (Brassard et al., 2002; Song, 2017; Soni & Rasool, 2021). The storage complexity showing qubits estimation for Approx.-QC and Exact-QC is also shown additionally in the presented Table 7.
- There are two cases to obtain the resulting complexities of combining the QC and GSO as it is further used in our simulation of EnQPBE algorithm – (1) Run Approx.-QC followed by the GSO to find all t occurrences of the pattern, so $\max(\sqrt{N} + \sqrt{Nt}) = O(\sqrt{Nt})$ time; and (2) Run Exact-QC followed by GSO to find all t occurrences of the pattern, therefore $\sqrt{Nt} + \sqrt{Nt} = 2 \times \sqrt{Nt} = O(\sqrt{Nt})$ time. Therefore, the complexity is still bounded by $O(\sqrt{Nt})$ time (Brassard et al., 2002; Lomont, 2003; Song, 2017). Similarly for these cases, the complexity of EnQBCEA algorithm remains $O(\sqrt{tt'})$ time as it works on t filtered indices to find t' pattern occurrences (Brassard et al., 2002; Soni & Rasool, 2021).
- We may expect accurate number of GSO iterations when the exact value of t is obtained through Exact-QC but the deviations in t values are possible through Approx.-QC algorithm, and hence the quantum search results need to be compromised with more errors.

Design and analysis of algebraic normal form to realize QMEM

To simulate our algorithms with the effective quantum processing framework, we propose the design of an algebraic normal form (ANF) circuit for realizing QMEM. Thus, this supports the hybrid simulation (Bogdanova et al., 2018; Hao et al., 2020). We can implement and perform most of the quantum operations directly by utilizing the

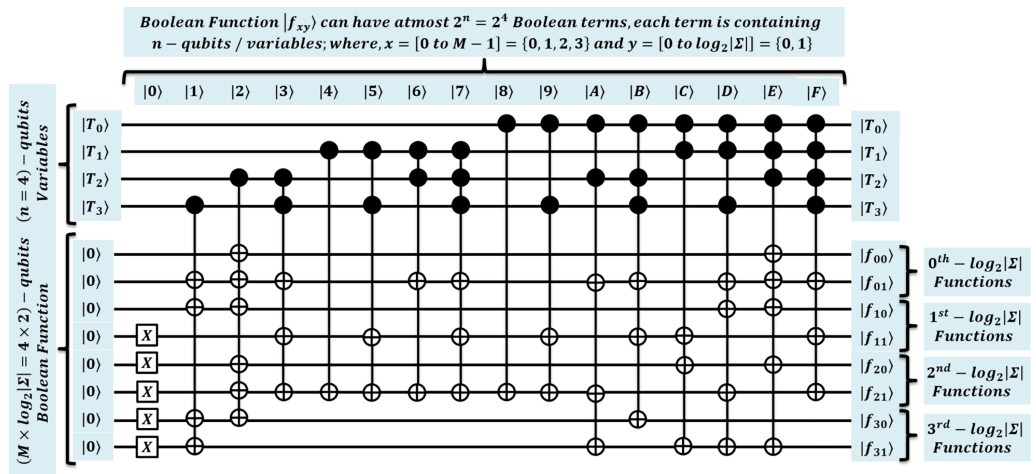


Figure 8 Quantum algebraic normal form (ANF) circuit used to realize QMEM processing.

Full-size DOI: 10.7717/peerj-cs.957/fig-8

advantage of ANF that are equivalent to unitary circuits, such as U_{Load} (QMEM transformation), U_{Comp} (QEM operation), and needful quantum adder operation (QAF filtering); hence, this saves the qubits requirement (Malviya & Tiwari, 2020; Malviya & Tiwari, 2021). The other requisite circuits and GSO operations needed for our proposed algorithms will be implemented using combination of ANF and the specific quantum unitary operations available in the QuEST library (defined in next section, used for simulation purpose). For comprehensive understanding of the ANF based QMEM realization refer to Malviya & Tiwari (2020); Soni & Rasool (2021); Soni & Malviya (2021) and Malviya & Tiwari (2021). We proposed a quantum circuit in Fig. 8 showing implicit operational method about the memory processing mentioned in Fig. 2.

A design of QMEM transformation is proposed here for a main unitary U_{Load} by using ANF. This will be later used in the next section to simulate QMEM. So, for considered $|T_{2^n \times w}\rangle_{\text{QMEM}}$, the quantum circuit of Fig. 8 creates a superposition of $N = 2^n$ text addresses by applying $H^{\otimes n}$ gates on n qubits address register $|T_i\rangle_{\text{QA}}$. These n qubits are used in ANF as n variables to form 2^n possible binary strings, usually called Boolean terms. In Fig. 8, the $n = 4$ variables are taken as $|T_0 T_1 T_2 T_3\rangle$, where $|T_0\rangle = |2^3\rangle$ and $|T_3\rangle = |2^0\rangle$ are the most significant and least significant qubit positions. Therefore, the total $2^4 = 16$ possible terms $\{|0\rangle \dots, |7\rangle, \dots, |F\rangle\}$ forms uniform superposition of binary strings $\{|0000\rangle \dots, |0111\rangle, \dots, |1111\rangle\}$.

Further, ANF creates the data superposition, by realizing all the substring data load operation in parallel, each of size $M \times \log_2|\Sigma|$ in entangled data register $|T_{[i]}\rangle_{\text{QD}}$ for each $|T_i\rangle_{\text{QA}}$. So, for such realization, $M \times \log_2|\Sigma|$ Boolean functions are computed in parallel, each can have at most $O(2^n)$ Boolean terms. These terms are computed with the logical “AND” followed by “XOR” operations. The computation of all possible terms, results output of associated Boolean function. A circuit is shown in Fig. 8 (about Fig. 2) considers pattern of length $M = 4$. Therefore, total 4×2 Boolean functions

Table 8 Simulation detail to realize the design of quantum effective processing framework.

Simulation of QMEM				Simulation of QEM				Simulation of GSO			
Concept used	Circuit realized	Qubits used	Circuit depth	Concept used	Circuit realized	Qubits used	Circuit depth	Concept used	Circuit realized	Qubits used	Circuit depth
ANF based circuit (Fig. 8)	U_{QMEM} , U_{Load}	$n + w$ or $tq + w$	$O(2^{tq})$ $tq \leq n$	Boolean Oracle circuit	U_{Comp}	$2 \times w$	$O(1)$	Phase Oracle circuit	U_{Mark} , U_{Diff}	$n + 1$ or $tq + 1$	$O(\sqrt{2^{tq}})$ $tq \leq n$

$\{|f_{00}\rangle, |f_{01}\rangle, |f_{10}\rangle, |f_{11}\rangle, |f_{20}\rangle, |f_{21}\rangle, |f_{30}\rangle, |f_{31}\rangle\}$ are computed in parallel as shown in Eqs. (9)–(16) (Bogdanova et al., 2018; Malviya & Tiwari, 2020).

$$|f_{00}\rangle = T_2 \oplus T_0 T_1 T_2 \quad (9)$$

$$|f_{01}\rangle = T_3 \oplus T_2 \oplus T_2 T_3 \oplus T_1 T_2 \oplus T_1 T_2 T_3 \oplus T_0 T_2 \oplus T_0 T_2 T_3 \oplus T_0 T_1 T_3 \oplus T_0 T_1 T_2 \oplus T_0 T_1 T_2 T_3 \quad (10)$$

$$|f_{10}\rangle = T_3 \oplus T_2 \oplus T_0 T_1 T_3 \oplus T_0 T_1 T_2 \quad (11)$$

$$|f_{11}\rangle = 1 \oplus T_2 T_3 \oplus T_1 T_3 \oplus T_1 T_2 T_3 \oplus T_0 T_3 \oplus T_0 T_2 T_3 \oplus T_0 T_1 \oplus T_0 T_1 T_2 T_3 \quad (12)$$

$$|f_{20}\rangle = 1 \oplus T_2 \oplus T_0 T_1 \oplus T_0 T_1 T_2 \quad (13)$$

$$|f_{21}\rangle = 1 \oplus T_2 \oplus T_2 T_3 \oplus T_1 \oplus T_1 T_3 \oplus T_1 T_2 \oplus T_1 T_2 T_3 \oplus T_0 \oplus T_0 T_3 \oplus T_0 T_2 \oplus T_0 T_1 T_3 \oplus T_0 T_1 T_2 T_3 \quad (14)$$

$$|f_{30}\rangle = 1 \oplus T_3 \oplus T_2 \oplus T_0 T_2 T_3 \quad (15)$$

$$|f_{31}\rangle = 1 \oplus T_3 \oplus T_0 T_2 \oplus T_0 T_1 \oplus T_0 T_1 T_3 \oplus T_0 T_1 T_2 \quad (16)$$

Each function $|f_{xy}\rangle$ with $x = [0 \text{ to } M - 1] = \{0, 1, 2, 3\}$ and $y = [0 \text{ to } \log_2|\Sigma|] = \{0, 1\}$ is computed using variables associated with each term. To load all substring of size $M \times \log_2|\Sigma|$ in $|T_{[i]}\rangle_{\text{QD}}$ for each text address $|T_i\rangle_{\text{QA}}$ in superposition, the binary string equivalent to index position $|T_i\rangle$ is taken as input, and by applying their instances, these Boolean functions are then computed to generate the desired substring within superposition. For example, the loading of text substring indexed at $|T_4\rangle_{\text{QA}}$, uses binary string $|0100\rangle_{\text{QA}}$ to load the desired output string in data register $|00011011\rangle_{\text{QD}}$ (see Fig. 2). This realization facilitates the qubits consuming operation in parallel, and thus, it simulates the quantum algorithms with the minimum qubits requirement (Malviya & Tiwari, 2020; Soni & Rasool, 2021; Soni & Malviya, 2021; Malviya & Tiwari, 2021). The design specifications used for quantum effective processing of algorithms are specified in Table 8 along with interpretation. Later, we will use these designs to simulate our proposed quantum algorithms using the QuEST simulation.

Design specifications used for quantum effective processing framework:

- Table 8 specifies the proposed designs of quantum effective processing framework. It is used in reference with Table 4 to know the quantum gates required for circuit, processing time and qubits needed to realize a circuits.
- The ANF circuit is realized as equivalent unitary U_{Load} (Eq. 3) for QMEM transformation. A circuit implementation needs quantum gates set

$\{H^{\otimes tq}, C^{tq}NOT, X^{\otimes tq}\}$ with $(tq \leq n)$. Such circuit can be simulated later with varying length, as per needed size of QMEM to realize.

- The time complexity of ANF based QMEM depends on the circuit depth constructed over tq input variables $tq \leq n$. It realizes $M \times \log_2|\Sigma|$ Boolean function in parallel, each consist of at most 2^{tq} terms. So, with maximum circuit depth, this circuit will take the exponential complexity $O(2^{tq})$ as $tq \leq n$ under the simulation. We conclude that the physical QMEM processing is remarkable with $O(1)$ time; however, it is exponentially slow in classical.
- The $O(1)$ time QEM $\approx U_{\text{Comp}}$ (Eq. 5) design can be simulated efficiently with $M \times \log_2|\Sigma|$ qubits as all substrings, each of $M \times \log_2|\Sigma|$ length, can realize in superposition using ANF.
- The GSO can be realized as per Table 4. A unitary U_{Mark} (Eq. 7) marks index with the phase inversion through $(C^{tq-1}NOT)$ gate, this flips a target index by inverting ancilla. Further, amplification circuit is used with the set of gates $\{\{H^{\otimes tq}, X^{\otimes tq}\}C^{tq-1}Z, \{X^{\otimes tq}, H^{\otimes tq}\}\}$ (Broda, 2016; Figgatt et al., 2017; Coles, 2020). A circuit depth of GSO is $O(\sqrt{2^{tq}})$, so this depends on text size, as for t sized filtered or N sized original text with $t \leq N$.

SIMULATION AND EXPERIMENTAL DETAIL

Our proposed algorithms are validated using hybrid (classical and quantum) simulation for the effective realization of equivalent quantum circuits. Therefore, we implemented the algorithms by utilizing the advantage of a C-Library based, flexible simulator with a multi-platform support, called the Quantum Exact Simulation Toolkit (QuEST) (Jones & Benjamin, 2018). We do not intend to analyze the simulation efficiency because of quantum operational restrictions on the classical machine. For a detailed study of QuEST simulation, refer to the published articles (Jones & Benjamin, 2018; Malviya & Tiwari, 2020; Malviya & Tiwari, 2021; Soni & Rasool, 2021; Soni & Malviya, 2021).

QuEST specific simulation features and environment setting

Quantum computations are highly complex, and their efficient simulation on the classical machine is not expected rather than the quantum machine. We performed the simulation to analyze the feasibility of quantum algorithm computations. A quantum machine with a significant amount of qubits still does not exist to realize quantum algorithms. Therefore, we used the QuEST library for the efficient and high-performance simulation of quantum circuits as a substitute for the quantum computer. This simulator is ideal, open-source and available with competent hybrid features such as multithreaded, distributed, and GPU accelerated to use classical hardware for the efficient simulation of quantum circuits. The QuEST simulator proved for the excellent scaling on multicore architectures. Hybrid features of this simulator realized in parallel execution support of OpenMP and MPI. We expect no compromise on simulating the quantum computations even realization is more accurate on a single node, shared memory and distributed systems. A QuES simulation prepares basic and multi-controlled quantum gates as either

pure state (vectors) or mixed state (density matrix) under the presence of decoherence (Jones & Benjamin, 2018). This simulation is effective as it performs the quantum operations in the absence of quantum noise.

In their article, Jones & Benjamin (2018), presented the performance comparison of QuEST with the other simulators, and they justified that QuEST is effective because it speeds up simultaneous quantum operations by data parallelism with SIMD execution support. The GPU acceleration is possible through NVIDIA's CUDA to attain operational speedup and to facilitate parallelism in quantum specific scientific codes. This maintains exponential operations (2^n) as the pure quantum state over n -qubits quantum register represented as complex floating-point numbers with default double precision. The quantum multicore realization is the implicit phenomenon that is implemented through the QuEST simulator in the separate quantum execution environment. However, such realization is based on parallel execution of the task in the multithreaded environment over the multiple cores of the CPU (Jones & Benjamin, 2018). Conclusively, we used the QuEST for high-performance simulation of quantum circuits and effective implementation equivalent to quantum algorithms.

We perform the experiments by implementing our quantum algorithms locally on one node with the machine configuration as "Intel i7-7700HQ" processor (having four cores and eight threads) running at 2.80 GHz (having 2400 MHz clock frequency) and 8GB classical RAM (CRAM). We set the QuEST execution environment for either a single or multiple (three) quantum system, each of them contains a separate register with a set of qubits in a pure state to show simulation of our quantum algorithms on single and multicore architecture. The simulation features such as OpenMP is enabled, GPU acceleration is disabled and default double-precision size of 8 bytes is used for reading probability amplitudes; however, the hybrid simulation would be effective.

Description and encoding of biological dataset and patterns

For the simulation purpose, we used the gene sequence database of "Severe Acute Respiratory Syndrome Corona-Virus 2 SARS-CoV-2" for humans. A detailed dataset description and QuEST specific simulation codes are specified within subsection of Additional Information and Declarations entitled "Data and Simulation Codes Availability".

An idea of implementation is to assign each symbol of the alphabet set Σ with the binary string of length $\log_2|\Sigma|$ qubits, and then to transform text database and pattern into binary encoded form. The nucleotide/gene/genome sequence database is preferred for validating our algorithms, so each DNA character of $\Sigma = \{A, T, C, G\}$ is assigned with the $\log_2 4 = 2$ length binary string as $\Sigma = \{00, 01, 10, 11\}$ (Faro & Lecroq, 2009; Soni & Rasool, 2021; Soni & Malviya, 2021). In contrast, the peptide sequences/protein databases with amino acid symbols set $|\Sigma| = 20$ are ignored here to avoid simulation specific restricted processing of long length binary strings $\log_2|\Sigma| = 5$ qubits, as this increases qubits requirement.

The subsets of gene sequence (SARS – CoV – 2) is intentionally prepared, as per feasibility of simulation with the text file sizes of $\{128, 256, 512\}$ characters. A QPU with

$C = 3$ cores is used to realize a case ($m \leq C$) for single pattern $|P| = 1$ and multiple patterns set $|P| = 3$. In case of single pattern, other cores will remain idle. A possible case of ($m > C$) is shown by taking multiple patterns set $|P| = 6$. For ($m = C$) case, we take each pattern as of equal size by considering “open reading frame search – patterns” used in the codon process, thus, the pattern of length $\{3, 3, 3\}$ characters is taken as $\{TAA, TAG, TGA\}$ to identify stop codon. And for ($m > C$) case, the 3 length patterns $\{TAA, TTT, TAG, TAC, TGA, TGC\}$ are searched using a multicore environment. Next, we take unequal sized patterns $\{TA, TAG, TGAC\}$ to realize ($m = C$) case by considering the DNA regular expression based “motif patterns” of length $\{2, 3, 4\}$ characters. For ($m > C$) case, we take the pattern of length $\{2, 2, 3, 3, 4, 4\}$ characters as $\{TA, TC, TAG, TTC, TGAC, TTCA\}$. The restricted singleton set $|P| = 1$ is used to search single pattern $\{ATG\}$ (start codon of frame) for existing algorithms. Text and pattern are encoded in binaries, but we specify our results with character file sizes. For each $QCore_c$, we take the pattern of $M_k \times \log_2|\Sigma|$ qubits, and sequence text of size $N = 2^n$ indices with word length $\log_2|\Sigma|$ qubits. Exact pattern match is performed by exploring text on QMEM (realized by ANF), and by applying QEM circuit for comparing $M \times \log_2|\Sigma|$ qubits in parallel.

SIMULATION RESULTS AND DISCUSSION

Our proposed algorithms EnQPBEA-MPM and EnQBCEA-MPM were simulated using the QuEST simulator. The experimental results observed during QuEST specific simulation are discussed here in the initial section. In the next section, we suggest some applications related to biological sequence processing for our proposed algorithms.

Simulation detail and analysis with algorithms evaluation criteria

The qubits estimation of a quantum algorithm (or equivalent quantum circuit) shows simulation possibility; however, actual qubits requirement with multiplicative constants decides, whether it is feasible or not. Thus, the performance of QuEST simulation depends on the scaling of multiplicative factors with respect to the data (qubits) processing requirement of quantum circuits. An excessive qubits requirement also limit an underlying configuration of a classical machine. This increases the CRAM workspace and classical CPU processing time with exponential increase. In general, a complete human genome sequence can be excessively large as of (2^{30}) nucleotide characters with approximately (3×10^9) base pairs which are contained in 23 chromosomes, each contains gene sequence of at least (2^{15}) DNA/RNA characters (Faro & Lecroq, 2013; Neamatollahi, 2020; Zou et al., 2015). So, for a simulation of n qubits system, QuEST realizes 2^n variables (each need 8 bytes of double precision) in $O(2^n)$ classical processing time. Therefore, CRAM and a classical CPU processing time proportionally increase as with qubits requirement. For this reason, we prepared the subsets of gene sequence (SARS-CoV-2) with text file sizes of $\{128, 256, 512\}$ characters by analyzing the feasible QuEST based hybrid simulation of QPU with C quantum cores accessing text T of size N on shared QMEM.

ANF is actually implemented to simulate the QMEM behaviour and for the other requisite operations. Therefore, in reference to the interpretation of Table 8, we simulate

the ANF circuit with varying length and as per needed size of QMEM to realize. However, based on ANF the QuEST simulation of QMEM is observed exponentially slow. The most important point to remember is justified here, that the ANF-based QMEM circuit allows several quantum operations with no increase in qubits requirement. In experimental results, we may observe some deviations and exceptions (if identified) due to implicit random increase in depth of Boolean functions as they are used to simulate QMEM. Further, we use this to perform other requisite quantum operations on the same ANF circuit.

We used two implementations of Boolean oracle circuit for $QEM \approx U_{Comp}$ (Eq. 5). First, using $\log_2|\Sigma|$ sized ancilla qubits to store matching results of each index. Next, we use QuEST specific complex-matrix unitary to find a match and to negate the index for marking. Similarly, the simulation of GSO is realized as per Tables 4 and 8, however, QuEST specific multi-controlled qubit unitary is used to implement the phase inversion.

The QuEST simulator realizes exponential operations effectively by optimizing simulation performance on the classical machine. This simulator provides the log file of quantum assembly instructions (QASM) which help us to record the operations executed on quantum registers by quantum gates and to report execution time of specific quantum circuit during simulation (Jones & Benjamin, 2018; Malviya & Tiwari, 2020; Malviya & Tiwari, 2021; Soni & Malviya, 2021). A CRAM is allocated on demand, so its workspace area may contain several blocks of memory and may be available in compressed form. So, in addition, we used process explorer to measure the maximum workspace requirement of CRAM during the execution of a simulated algorithm.

QuEST specific algorithmic simulation results with observation

This section includes QuEST simulation with observation to map our theoretical – experimental results of algorithms. The results are categorized separately for equal and unequal sized patterns. We noted the results in the tables as per the analysis cases ($m \leq C$) and ($m > C$) for different text file sizes. A recorded execution log is mentioned in Tables 9 and 10. To prevent the overshooting problem of GSO we implemented exact and approximate quantum counting (QC) algorithms that can find the required number of GSO iterations. So, the observed results of QC and further error analysis are included from Tables 11–13 (for equal sized pattern) and from Tables 14–16 (for unequal sized pattern). The average search time with the memory requirement of the algorithm under QuEST simulation is noted in Tables 17 and 18.

Analysis of the experimental log observed during QuEST simulation:

- For our algorithms EnQPBEA-MPM and EnQBCEA-MPM, Tables 9 and 10 are used to categorize the results between separate text file sizes {128, 256, 512} and analysis cases ($m \leq C$) and ($m > C$) are formed for equal – unequal sized multiple pattern set $P = \{P_1, P_2, P_3, P_4, P_5, P_6\}$ of lengths {3, 3, 3, 3, 3, 3} and {2, 2, 3, 3, 4, 4}. A QPU with quantum cores $C = \{C_1, C_2, C_3\}$ is considered for the separate execution of desired pattern search.

Table 9 Observed outcomes of experimental log during QuEST simulation for equal sized patterns.

Quantum algorithm	Analysis case	Search pattern	Text file size: 128					Text file size: 256					Text file size: 512							
			Qubits noted	Quantum gates needed					Qubits noted	Quantum gates needed					Qubits noted	Quantum gates needed				
				H	X	R_z	CZ	CX		H	X	R_z	CZ	CX		H	X	R_z	CZ	CX
EnQPBEA-MPM	$(m \leq C)$	C P:ATG	17	91	95	141	6	141	18	88	91	265	5	265	19	63	65	545	3	545
		C1 P1:TAA	17	63	65	141	4	142	18	104	105	265	6	266	19	63	63	545	3	546
		C2 P2:TAG	17	63	67	141	4	142	18	136	139	265	8	266	19	117	119	545	6	546
	$(m > C)$	C3 P3:TGA	17	91	95	141	6	142	18	136	139	265	8	266	19	81	83	545	4	546
		C1 P1:TAA	17	63	65	141	4	142	18	104	105	265	6	266	19	63	63	545	3	546
		C2 P2:TTT	17	21	25	141	1	142	18	56	59	256	3	266	19	45	47	545	2	546
		C3 P3:TAG	17	63	67	141	4	142	18	136	139	265	8	266	19	117	119	545	6	546
		C1 P4:TAC	17	49	52	141	3	142	18	56	58	265	3	266	19	63	64	545	3	546
		C2 P5:TGA	17	91	95	141	6	142	18	136	139	265	8	266	19	81	83	545	4	546
		C3 P6:TGC	17	63	68	141	2	142	18	120	124	265	7	266	19	99	102	545	5	546
EnQBCEA-MPM	$(m \leq C)$	C P:ATG	14+5	54	39	308	4	308	16+6	50	36	441	3	442	18+7	53	28	2,366	2	2,366
		C1 P1:TAA	14+5	49	37	598	3	600	16+6	70	56	1,446	4	1,448	18+7	53	37	3,084	2	3,086
		C2 P2:TAG	14+2	24	15	598	2	600	16+3	31	20	1,450	2	1,452	18+4	38	25	3,142	2	3,144
	$(m > C)$	C3 P3:TGA	14+0	14	6	577	0	578	16+1	19	9	1,169	0	1,171	18+4	38	24	2,785	2	2,787
		C1 P1:TAA	14+5	49	37	598	3	600	16+6	70	56	1,446	4	1,448	18+7	53	37	3,084	2	3,086
		C2 P2:TTT	14+7	49	28	7	2	9	16+8	88	64	8	4	10	18+9	81	54	9	3	11
		C3 P3:TAG	14+2	24	15	598	2	600	16+3	31	20	1,450	2	1,452	18+4	38	25	3,142	2	3,144
		C1 P4:TAC	14+3	39	27	488	2	490	16+4	46	32	1,152	2	1,154	18+5	53	37	3,082	2	3,084
		C2 P5:TGA	14+0	14	6	577	0	578	16+1	19	9	1,169	0	1,171	18+4	38	24	2,785	2	2,787
		C3 P6:TGC	14+1	49	30	483	3	485	16+2	79	56	1,010	4	1,012	18+3	67	42	2,065	3	2,067

- We assume $|P| = 1$ for $((m = 1) < (C = 3))$ to search for single pattern P of length $\{3\}$ on $|C| = 1$ i.e. single core to show the simulation of existing QPBE and QBCE algorithms. In this case, other cores are remaining idle. The case of $((m = 3) = (C = 3))$ is considered for searching the desired pattern on individual quantum core. We noted the performance of our algorithms for the case $((m = 6) > (C = 3))$ to realize their executions for large number of patterns (exactly doubled) on constant number of quantum cores. For these cases, we utilized QuEST specific log file that contains a record of standard QASM instructions.
- The log record for EnQPBEA and EnQBCEA algorithms are identified for searching, but in case of the EnQBCEA algorithm, the filtering log is additionally recorded. It keeps number of quantum gates needed during the simulation of the quantum algorithm or its equal quantum circuit. A universal quantum gates set $\{H, X, R_z, C^{tq-1}Z, C^{tq}X\}$ is noted in QASM log. We used to represent $C^{tq-1}Z$ and $C^{tq}X$ as CZ and CX to save the text space in tables. The number of coded qubits is observed additionally during a simulation of algorithm within test log.

Table 10 Observed outcomes of experimental log during QuEST simulation for unequal sized patterns.

Quantum algorithm	Analysis case	Search pattern	Text file size: 128					Text file size: 256					Text file size: 512							
			Qubits noted	Quantum gates needed					Qubits noted	Quantum gates needed					Qubits noted	Quantum gates needed				
				H	X	Rz	CZ	CX		H	X	Rz	CZ	CX		H	X	Rz	CZ	CX
EnQPBEA-MPM	$(m \leq C)$	C P:ATG	17	91	95	141	6	141	18	88	91	265	5	265	19	63	65	545	3	545
		C1 P1:TA	15	21	23	141	1	142	16	40	41	265	2	266	17	27	27	545	1	546
		C2 P2:TAG	17	63	67	141	4	142	18	136	139	265	8	266	19	117	119	545	6	546
		C3 P3:TGAC	19	91	96	141	6	142	20	200	204	265	12	266	21	225	228	545	12	546
	$(m > C)$	C1 P1:TA	15	21	23	141	1	142	16	40	41	265	2	266	17	27	27	545	1	546
		C2 P2:TC	15	35	38	141	2	142	16	40	42	265	2	266	17	45	46	545	2	546
		C3 P3:TAG	17	63	67	141	4	142	18	136	139	265	8	266	19	117	119	545	6	546
		C1 P4:TTC	17	49	53	141	3	142	18	72	75	265	4	266	19	63	65	545	3	546
		C2 P5:TGAC	19	91	96	141	6	142	20	200	204	265	12	266	21	225	228	545	12	546
		C3 P6:TTCA	19	91	95	141	6	142	20	120	123	265	7	266	21	99	101	545	5	546
EnQBCEA-MPM	$(m \leq C)$	C P:ATG	14+5	54	39	308	4	308	16+6	50	36	441	3	442	18+7	53	28	2,366	2	2,366
		C1 P1:TA	14+5	29	17	598	1	600	16+6	46	32	1,446	2	1,448	18+7	39	23	3,084	1	3,086
		C2 P2:TAG	14+2	24	15	598	2	600	16+3	31	20	1,450	2	1,452	18+4	38	25	3,142	2	3,144
		C3 P3:TGAC	14+0	14	6	523	0	524	16+0	16	7	1,193	0	1,194	18+0	9	3	861	0	863
	$(m > C)$	C1 P1:TA	14+5	29	17	598	1	600	16+6	46	32	1,446	2	1,448	18+7	39	23	3,084	1	3,086
		C2 P2:TC	14+5	63	42	435	3	437	16+6	72	48	974	3	976	18+7	81	54	1,955	3	1,957
		C3 P3:TAG	14+2	24	15	598	2	600	16+3	31	20	1,450	2	1,452	18+4	38	25	3,142	2	3,144
		C1 P4:TTC	14+5	77	56	423	4	425	16+6	104	80	896	5	898	18+7	99	72	1,791	4	1,793
		C2 P5:TGAC	14+0	14	6	523	0	524	16+0	16	7	1,193	0	1,194	18+0	9	3	861	0	863
		C2 P6:TTCA	14+3	54	45	443	4	445	16+4	70	55	1,109	4	1,111	18+5	67	50	2,667	3	2,669

- In reference to [Table 6](#), we simulated the EnQPBEA algorithm using workspace qubits. Instead of actual qubits $(n + 2 \times (M \log_2 |\Sigma|) + 1)$, the $(n + M \log_2 |\Sigma| + 2 + 2)$ qubits used in the implementation. Here, all text substrings of size $M \log_2 |\Sigma|$ are realized using ANF, and $\log_2 |\Sigma| = 2$ workspace qubits store the parallel matching result of each index in superposition. Other two qubits are used as ancillary to support GSO operation. Our findings on qubits, for both the equal and unequal sized patterns, are observed the same as expectations.
- The simulation of EnQBCEA algorithm is efficiently coded with $(2n + tq)$ qubits instead of the actual $(2n + 2 \times (M \log_2 |\Sigma|) + tq + 1)$ qubits mentioned in [Table 6](#). We took $2n$ qubits for QAF filtering, and tq qubits to search on filtered indices. All substring of size $M \log_2 |\Sigma|$ are realized using ANF and the pattern is loaded classically. For GSO operation, QuEST unitary complex-matrix is used to find a match and to negate the index for marking. The qubits are observed as the same as expectations for both equal and unequal sized patterns.
- We wished to show the implementation using QPU with C quantum cores; thus, the QuEST execution environment was initialized as either a single or multiple (three) quantum system containing a separate register set. We coded hybrid simulation to

Table 11 Observed results of QC with error analysis in QuEST simulation for $N = 128$ & equal sized patterns.

Quantum algorithm	Analysis case	Search pattern	Text file size: 128										
			Actual patterns	Filtered indices	Error analysis (Exact-QC)				Error Analysis (Approx. -QC)				
					Exact QC	No. of CIP	No. of IIP	Error %	Approx. QC	No. of CIP	No. of IIP	Error %	
EnQPBEA-MPM	$(m \leq C)$	C P:ATG	1	–	1	842	158	15.8	1	836	164	16.4	
		C1 P1:TAA	2	–	2	926	74	7.4	1	853	147	14.7	
		C2 P2:TAG	2	–	2	923	77	7.7	1	898	102	10.2	
		C3 P3:TGA	1	–	1	855	145	14.5	1	846	154	15.4	
	$(m > C)$	C1 P1:TAA	2	–	2	918	82	8.2	1	863	137	13.7	
		C2 P2:TTT	10	–	10	850	150	15	11	801	199	19.9	
		C3 P3:TAG	2	–	2	919	81	8.1	1	877	123	12.3	
		C1 P4:TAC	4	–	4	873	127	12.7	5	804	196	19.6	
		C2 P5:TGA	1	–	1	856	144	14.4	1	852	148	14.8	
		C3 P6:TGC	2	–	2	912	88	8.8	1	825	175	17.5	
EnQBCEA-MPM	$(m \leq C)$	C P:ATG	1	3	1	923	77	7.7	1	914	86	8.6	
		C1 P1:TAA	2	23	2	953	47	4.7	1	592	408	40.8	
		C2 P2:TAG	2	4	2	509	491	49.1	2	501	499	49.9	
		C3 P3:TGA	1	1	1	1,000	0	0	1	1,000	0	0	
	$(m > C)$	C1 P1:TAA	2	23	2	969	31	3.1	1	883	117	11.7	
		C2 P2:TTT	10	128	10	887	113	11.3	10	867	133	13.3	
		C3 P3:TAG	2	4	2	536	464	46.4	2	511	489	48.9	
		C1 P4:TAC	4	5	4	736	264	26.4	3	654	346	34.6	
		C2 P5:TGA	1	1	1	1,000	0	0	1	1,000	0	0	
		C3 P6:TGC	2	2	2	1,000	0	0	2	1,000	0	0	

intentionally save qubits, such that, qubits requirement on any core should not exceed the limits of a classical machine.

- Especially for searching, the qubits needed by EnQPBEA is comparatively more than the EnQBCEA because of search is performed with original indices rather than filtered. A QAF takes $2n$ qubits to filter t indices, so, $\log_2 t = tq$ search qubits may vary as per t value. The expansion of different text search space with reduced indices enhances search mechanism, but this would happen, when a value of t is found as too low as likely the value of $\log_2 N = n$.
- The qubits needed for the searching increases in accordance with the size of the biological text sequence and in direct proportion to the varying length patterns. This phenomenon can be observed in the tables by analysing noted qubits for both equal – unequal sized patterns and text size. A QuEST simulation of algorithms on quantum multicore architecture shows that quantum registers are separately allocated with a set of qubits in the pure state.
- We observed the quantum logic gates as implicitly realized under the QuEST simulation of algorithms. For EnQPBEA with equal – unequal sized patterns running on any

Table 12 Observed results of QC with error analysis in QuEST simulation for $N = 256$ and equal sized patterns.

Quantum algorithm	Analysis case	Search pattern	Text file size: 256											
			Actual patterns	Filtered indices	Error analysis (Exact-QC)				Error analysis (Approx. -QC)					
					Exact QC	No. of CIP	No. of IIP	Error %	Approx. QC	No. of CIP	No. of IIP	Error %		
EnQPBEA-MPM	$(m \leq C)$	C P:ATG	5	-	5	873	127	12.7	6	818	182	18.2		
		C1 P1:TAA	4	-	4	955	45	4.5	6	869	131	13.1		
		C2 P2:TAG	2	-	2	944	56	5.6	2	935	65	6.5		
		C3 P3:TGA	2	-	2	867	133	13.3	2	867	133	13.3		
	$(m > C)$	C1 P1:TAA	4	-	4	962	38	3.8	6	888	112	11.2		
		C2 P2:TTT	16	-	16	886	114	11.4	15	811	189	18.9		
		C3 P3:TAG	2	-	2	952	48	4.8	2	971	29	2.9		
		C1 P4:TAC	10	-	10	906	94	9.4	10	905	95	9.5		
		C2 P5:TGA	2	-	2	888	112	11.2	2	894	106	10.6		
		C3 P6:TGC	3	-	3	943	57	5.7	2	901	99	9.9		
		EnQBCEA-MPM	$(m \leq C)$	C P:ATG	5	9	5	925	75	7.5	2	505	495	49.5
				C1 P1:TAA	4	47	4	968	32	3.2	5	915	85	8.5
C2 P2:TAG	2			7	2	984	16	1.6	2	983	17	1.7		
C3 P3:TGA	2			2	2	1,000	0	0	2	1,000	0	0		
$(m > C)$	C1 P1:TAA		4	47	4	972	28	2.8	5	909	91	9.1		
	C2 P2:TTT		16	256	16	901	99	9.9	15	882	118	11.8		
	C3 P3:TAG		2	7	2	978	22	2.2	2	980	20	2		
	C1 P4:TAC		10	13	10	852	148	14.8	7	595	405	40.5		
C2 P5:TGA	2	2	2	1,000	0	0	2	1,000	0	0				
C3 P6:TGC	3	3	3	1,000	0	0	3	1,000	0	0				

$QCore_c$. The quantum gates are close proximate values to the gate observed during a single pattern search on a single quantum core. In same context, the number of quantum gates, noted on each $QCore_c$ for EnQBCEA, are approximately doubled than single core.

- Due to small-sized equal or unequal pattern lengths, the observed number of gates for both the algorithms are analysed in close proximity. However, there is a proportional increase in the gates as with the increase in text file sizes and for the varying length patterns. There exist, huge difference between the gates observation of EnQPBEA and EnQBCEA because the gates observed for EnQBCEA are combined for both filtering and searching. The size of filtered text eventually increases or decreases multiplicity of quantum gates during simulation.
- In general, we observed that the simulation takes more quantum gates due to the realization of ANF and other requisite quantum operations. We distributed uniform workload on all cores under the multiple (three) quantum system containing a separate register set. Table 9 shows a case of $(m > C)$ for that the overlapping pattern $P_2 = TTT$ executed on core C_2 takes very less number of gates as due to the reduced

Table 13 Observed results of QC with error analysis in QuEST simulation for $N = 512$ and equal sized patterns.

Quantum algorithm	Analysis case	Search pattern	Text file size: 512											
			Actual patterns	Filtered indices	Error analysis (Exact-QC)				Error analysis (Approx. -QC)					
					Exact QC	No. of CIP	No. of IIP	Error %	Approx. QC	No. of CIP	No. of IIP	Error %		
EnQPBEA-MPM	$(m \leq C)$	C P:ATG	11	–	11	888	112	11.2	11	881	119	11.9		
		C1 P1:TAA	14	–	14	967	33	3.3	15	876	124	12.4		
		C2 P2:TAG	4	–	4	978	22	2.2	5	914	86	8.6		
		C3 P3:TGA	8	–	8	907	93	9.3	8	900	100	10		
	$(m > C)$	C1 P1:TAA	14	–	14	960	40	4	15	843	157	15.7		
		C2 P2:TTT	34	–	34	943	57	5.7	36	907	93	9.3		
		C3 P3:TAG	4	–	4	978	22	2.2	5	902	98	9.8		
		C1 P4:TAC	15	–	15	934	66	6.6	15	935	65	6.5		
		C2 P5:TGA	8	–	8	918	82	8.2	8	900	100	10		
		C3 P6:TGC	6	–	6	971	29	2.9	5	917	83	8.3		
		EnQBCEA-MPM	$(m \leq C)$	C P:ATG	11	18	11	974	26	2.6	9	923	77	7.7
				C1 P1:TAA	14	97	14	980	20	2	14	969	31	3.1
C2 P2:TAG	4			11	4	989	11	1.1	2	545	455	45.5		
C3 P3:TGA	8			10	8	814	186	18.6	7	799	201	20.1		
$(m > C)$	C1 P1:TAA		14	97	14	987	13	1.3	14	963	37	3.7		
	C2 P2:TTT		34	512	34	974	26	2.6	33	928	72	7.2		
	C3 P3:TAG		4	11	4	990	10	1	2	506	494	49.4		
	C1 P4:TAC		15	19	15	593	407	40.7	15	581	419	41.9		
	C2 P5:TGA		8	10	8	805	195	19.5	7	800	200	20		
	C3 P6:TGC		6	6	6	988	12	1.2	3	929	71	7.1		

depth of ANF circuit. However, we noted proportional increase in the gate counts as per the length and occurrences of search pattern. There is no increase in gate requirements because most of the quantum operations are coded under ANF and this actually saves the specific requirements of quantum gates.

- To considering all file sizes, we observed the same growth in the gate counts of R_z and $C^{tq}X$ with a gradual increase. A controlled phase flip gate $C^{tq-1}Z$ is used to perform the phase inversion on the occurrence identification of pattern over the index. A subset of $\{H, X\}$ gates are used as per necessity to realize QMEM or diffusion operator of GSO. Any exception other than that are always expected because of the quantum operations are applied over the random increase in depth of Boolean function which is realized in ANF such that $tq \leq n$.

Quantum counting (QC) results and error analysis during QuEST simulation:

- For our algorithms EnQPBEA-MPM and EnQBCEA-MPM, we categorize the results in tables between separate text file sizes $\{128, 256, 512\}$ and the analysis cases $(m \leq C)$ and $(m > C)$ formed for equal – unequal sized multiple pattern set

Table 14 Observed results of QC with error analysis in QuEST simulation for $N = 128$ and unequal sized patterns.

Quantum algorithm	Analysis case	Search pattern	Text file size: 128										
			Actual patterns	Filtered indices	Error analysis (Exact-QC)				Error analysis (Approx. -QC)				
					Exact QC	No. of CIP	No. of IIP	Error %	Approx. QC	No. of CIP	No. of IIP	Error %	
EnQPBEA-MPM	$(m \leq C)$	C P:ATG	1	–	1	842	158	15.8	1	836	164	16.4	
		C1 P1:TA	10	–	10	579	421	42.1	11	549	451	45.1	
		C2 P2:TAG	2	–	2	912	88	8.8	1	892	108	10.8	
		C3 P3:TGAC	1	–	1	826	174	17.4	1	814	186	18.6	
	$(m > C)$	C1 P1:TA	10	–	10	596	404	40.4	11	579	421	42.1	
		C2 P2:TC	8	–	8	904	96	9.6	11	582	418	41.8	
		C3 P3:TAG	2	–	2	924	76	7.6	1	890	110	11	
		C1 P4:TTC	3	–	3	891	109	10.9	5	572	428	42.8	
		C2 P5:TGAC	1	–	1	833	167	16.7	1	826	174	17.4	
		C3 P6:TTCA	1	–	1	855	145	14.5	1	834	166	16.6	
EnQBCEA-MPM	$(m \leq C)$	C P:ATG	1	3	1	923	77	7.7	1	914	86	8.6	
		C1 P1:TA	10	23	10	961	39	3.9	9	957	43	4.3	
		C2 P2:TAG	2	4	2	511	489	48.9	2	505	495	49.5	
		C3 P3:TGAC	1	1	1	1,000	0	0	1	1,000	0	0	
	$(m > C)$	C1 P1:TA	10	23	10	966	34	3.4	9	957	43	4.3	
		C2 P2:TC	8	21	8	943	57	5.7	9	903	97	9.7	
		C3 P3:TAG	2	4	2	509	491	49.1	2	503	497	49.7	
		C1 P4:TTC	3	19	3	980	20	2	4	961	39	3.9	
		C2 P5:TGAC	1	1	1	1,000	0	0	1	1,000	0	0	
		C3 P6:TTCA	1	7	1	939	61	6.1	3	854	146	14.6	

$P = \{P_1, P_2, P_3, P_4, P_5, P_6\}$ of lengths $\{3, 3, 3, 3, 3, 3\}$ and $\{2, 2, 3, 3, 4, 4\}$. A QPU with quantum cores $C = \{C_1, C_2, C_3\}$ is considered for the separate execution of desired pattern search. We noted the results of equal sized pattern from Tables 11–13 and unequal sized pattern from Tables 14–16.

- In reference to the earlier discussions on Grover's quantum search, initially we implemented our algorithms by assuming that the t number of search solutions (either unique or multiple solution) are already known, and therefore, the GSO iterations were also coded in advance. The case of GSO overshooting is considered as t number of search solutions are unknown. However, it leads to the unknown number of GSO iterations and hence the probability of success would be vanishingly small. So, we handle this by implementing QC algorithm.
- To analyze our results, we implemented quantum counting (QC) (Brassard et al., 2002; Nielsen & Chuang, 2010) to estimate the t number of search solutions in advance. We obtained accurate value of t by Exact-QC and estimated value of t through Approx.-QC methods. We know that QC is an amplitude estimation method, therefore, additional quantum register is used with required precision qubits to store the exact or

Table 15 Observed results of QC with error analysis in QuEST simulation for $N = 256$ and unequal sized patterns.

Quantum algorithm	Analysis case	Search pattern	Text file size: 256										
			Actual patterns	Filtered indices	Error analysis (Exact-QC)				Error Analysis (Approx. -QC)				
					Exact QC	No. of CIP	No. of IIP	Error %	Approx. QC	No. of CIP	No. of IIP	Error %	
EnQPBEA-MPM	$(m \leq C)$	C P:ATG	5	–	5	873	127	12.7	6	818	182	18.2	
		C1 P1:TA	19	–	19	665	335	33.5	18	602	398	39.8	
		C2 P2:TAG	2	–	2	955	45	4.5	2	952	48	4.8	
		C3 P3:TAGAC	1	–	1	868	132	13.2	1	861	139	13.9	
	$(m > C)$	C1 P1:TA	19	–	19	617	383	38.3	18	596	404	40.4	
		C2 P2:TC	20	–	20	946	54	5.4	22	901	99	9.9	
		C3 P3:TAG	2	–	2	961	39	3.9	2	952	48	4.8	
		C1 P4:TTC	9	–	9	922	78	7.8	10	907	93	9.3	
		C2 P5:TAGAC	1	–	1	880	120	12	1	872	128	12.8	
		C3 P6:TTCA	3	–	3	910	90	9	2	895	105	10.5	
EnQBCEA-MPM	$(m \leq C)$	C P:ATG	5	9	5	925	75	7.5	2	505	495	49.5	
		C1 P1:TA	19	47	19	975	25	2.5	19	964	36	3.6	
		C2 P2:TAG	2	7	2	989	11	1.1	2	973	27	2.7	
		C3 P3:TAGAC	1	1	1	1,000	0	0	1	1,000	0	0	
	$(m > C)$	C1 P1:TA	19	47	19	975	25	2.5	19	964	36	3.6	
		C2 P2:TC	20	44	20	954	46	4.6	19	914	86	8.6	
		C3 P3:TAG	2	7	2	962	38	3.8	2	962	38	3.8	
		C1 P4:TTC	9	47	9	982	18	1.8	9	977	23	2.3	
		C2 P5:TAGAC	1	1	1	1,000	0	0	1	1,000	0	0	
		C3 P6:TTCA	3	13	3	970	30	3	2	911	89	8.9	

approximate value of t as count. In Exact-QC, we measure the accurate value of t using the register with a precision size $\approx \log_2 N$ qubits, and we need the register with precision size $< \log_2 N$ qubits to measure the approximate value of t through Approx.-QC (Brassard et al., 2002; Nielsen & Chuang, 2010). So, we coded required qubits in additional register, respectively. After executing Exact-QC and Approx.-QC algorithms, values of t are obtained. And then the algorithm EnQPBEA executes $\pi/4 \left(\sqrt{N/t} \right)$ and EnQBCEA executes $\pi/4 \left(\sqrt{t/t'} \right)$ no. of GSO iterations to obtain relative search results. We include the error analysis with the exact value of t Exact-QC and with the approximate value of t (Approx.-QC) in Tables 11–16.

- For evaluating the accuracy of search results, we include error analysis with Exact-QC and Approx.-QC cases. So for each pattern, after obtaining the value of t from Exact-QC and Approx.-QC, we repeat EnQPBEA and EnQBCEA algorithms 10 times separately on the individual quantum core. Each repetition completes 100 iterations of algorithms, and after each iteration, we perform the measurement on each core to obtain the search result. Instead of taking the average of 10 times, we have noted the results from Tables 11–16 by taking a summation of 10 repeated executions (each

Table 16 Observed results of QC with error analysis in QuEST simulation for $N = 512$ and unequal sized patterns.

Quantum algorithm	Analysis case	Search pattern	Text file size: 512									
			Actual patterns	Filtered indices	Error analysis (Exact-QC)				Error Analysis (Approx.-QC)			
					Exact QC	No. of CIP	No. of IIP	Error %	Approx. QC	No. of CIP	No. of IIP	Error %
EnQPBEA-MPM	$(m \leq C)$	C P:ATG	11	–	11	888	112	11.2	11	881	119	11.9
		C1 P1:TA	42	–	42	696	304	30.4	43	667	333	33.3
		C2 P2:TAG	4	–	4	970	30	3	5	920	80	8
		C3 P3:TAGAC	1	–	1	902	98	9.8	1	904	96	9.6
	$(m > C)$	C1 P1:TA	42	–	42	623	377	37.7	43	612	388	38.8
		C2 P2:TC	29	–	29	963	37	3.7	30	952	48	4.8
		C3 P3:TAG	4	–	4	975	25	2.5	5	917	83	8.3
		C1 P4:TTC	14	–	14	967	33	3.3	15	935	65	6.5
		C2 P5:TAGAC	1	–	1	899	101	10.1	1	900	100	10
		C3 P6:TTCA	5	–	5	945	55	5.5	5	945	55	5.5
EnQBCEA-MPM	$(m \leq C)$	C P:ATG	11	18	11	974	26	2.6	9	923	77	7.7
		C1 P1:TA	42	97	42	984	16	1.6	39	911	89	8.9
		C2 P2:TAG	4	11	4	993	7	0.7	2	545	455	45.5
		C3 P3:TAGAC	1	1	1	1,000	0	0	1	1,000	0	0
	$(m > C)$	C1 P1:TA	42	97	42	971	29	2.9	39	900	100	10
		C2 P2:TC	29	71	29	979	21	2.1	28	947	53	5.3
		C3 P3:TAG	4	11	4	975	25	2.5	2	566	434	43.4
		C1 P4:TTC	14	75	14	987	13	1.3	14	989	11	1.1
		C2 P5:TAGAC	1	1	1	1,000	0	0	1	1,000	0	0
		C3 P6:TTCA	5	18	5	982	18	1.8	4	966	34	3.4

bifurcates the measurement result out of 100 iterations), and hence it is equivalently considered as 1,000 iterations.

- We define some requisite parameters which are evaluated for the error analysis purpose, out of 1,000 iterations, such as – (1) No. of Correctly Identified Patterns (CIP): No. of times the pattern identified correctly at the measured index; (2) No. of Incorrectly Identified Patterns (IIP): No. of times the pattern does not found at measured index; (3) No. of Incorrectly Missed Patterns (IMP): No. of times any of the correct pattern index could not be measured; and (4) Error % : $((\text{No. of IIP}/(\text{No. of CIP} + \text{No. of IIP})) \times 100)$.
- In each of the 10 repeated executions, we coded 100 iterations for sufficient be valuations. If the number of iterations were selected too small ≈ 25 iterations, then there would have been the chance of getting the No. of IMP in our evaluations. However, because of the sufficient iterations, we have not reported this case for any search pattern. Therefore, we assure that the likely indices are at least identified during the search phase of both EnQPBEA & EnQBCEA algorithms. We also justify the fact, that the increase in number of iterations also increases the accuracy of measuring all the likely

Table 17 Experimental realization of algorithms through QuEST specific simulation for equal sized pattern.

Quantum algorithm	Analysis case	Search pattern	Text file size: 128			Text file size: 256			Text file size: 512		
			Avg. ET (Sec)	CRAM WS (KiB)	No. of IP	Avg. ET (Sec)	CRAM WS (KiB)	No. of IP	Avg. ET (Sec)	CRAM WS (KiB)	No. of IP
EnQPBEA-MPM	$(m \leq C)$	C P:ATG	0.205	5,978	1	0.502	8,702	5	1.409	16,082	11
		C1 P1:TAA	0.132	5,955	2	0.513	8,690	4	1.312	16,087	14
		C2 P2:TAG	0.112		2	0.604		2	2.219		4
		C3 P3:TGA	0.145		1	0.613		2	1.622		8
	$(m > C)$	C1 P1:TAA	0.233	5,994	2	0.913	8,723	4	3.137	16,116	14
		P4:TAC			4			10			15
		C2 P2:TTT	0.212		10	1.042		16	3.115		34
		P5:TGA			1			2			8
		C3 P3:TAG	0.231		2	1.323		2	4.935		4
		P6:TGC			2			3			6
EnQBCEA-MPM	$(m \leq C)$	C P:ATG	0.024	3,661	1	0.099	4,422	5	0.907	7,478	11
		C1 P1:TAA	0.037	4,130	2	0.145	6,447	4	0.901	15,719	14
		C2 P2:TAG	0.027		2	0.126		2	0.888		4
		C3 P3:TGA	0.025		1	0.111		2	0.774		8
	$(m > C)$	C1 P1:TAA	0.066	4,336	2	0.295	6,592	4	2.051	16,198	14
		P4:TAC			4			10			15
		C2 P2:TTT	0.042		10	0.218		16	1.537		34
		P5:TGA			1			2			8
		C3 P3:TAG	0.052		2	0.244		2	1.675		4
		P6:TGC			2			3			6

indices. And it also reduces the possibility of pattern that may be incorrectly missed. Similarly, on taking too large number of iterations $\approx 1,000$ iterations, a possibility of getting No. of IMP will be removed completely, but the algorithm performance becomes worse than the classical equivalent algorithm.

- The quantum counting Exact-QC and Approx.-QC are executed 10 times and majority result is considered as correct count of t *i.e.* either accurate value of t or estimated value of t . The obtained value of t of Exact-QC are found accurate as per actual number of pattern occurrences. As expected, we analyzed the deviations in values of t obtained after executing Approx.-QC algorithm. Therefore, to measure EnQPBEA and EnQBCEA search results, Error % of Approx.-QC case would be comparatively more than the Exact-QC case.
- For the case $((m = 1) < (C = 3))$, we show the simulation of existing QPBE and QBCE algorithms. So, a single pattern P of length $\{3\}$ is searched on a single core with the values of t obtained from Exact-QC and Approx.-QC. In this case, other cores are remaining idle. For the case of $((m = 3) = (C = 3))$ and $((m = 6) > (C = 3))$, we executed Exact-QC and Approx.-QC algorithms on individual quantum cores. After obtaining the separate values of t , the algorithms EnQPBEA and EnQBCEA execute for

Table 18 Experimental realization of algorithms through QuEST specific simulation for unequal sized pattern.

Quantum algorithm	Analysis case	Search pattern	Text file size: 128			Text file size: 256			Text file size: 512		
			Avg. ET (in Sec)	CRAM WS (KiB)	No. of IP	Avg. ET (in Sec)	CRAM WS (KiB)	No. of IP	Avg. ET (in Sec)	CRAM WS (KiB)	No. of IP
EnQPBEA-MPM	$(m \leq C)$	C P:ATG	0.205	5,978	1	0.502	8,702	5	1.409	16,082	11
		C1 P1:TA	0.030	11,929	10	0.111	20,903	19	0.331	40,504	42
		C2 P2:TAG	0.112		2	0.618		2	2.232		4
		C3 P3:TGAC	0.468		1	2.404		1	10.436		1
	$(m > C)$	C1 P1:TA	0.134	12,484	10	0.538	20,960	19	2.058	40,578	42
		P4:TTC			3			9			14
		C2 P2:TC	0.619		8	3.386		20	13.036		29
		P5:TGAC			1			1			1
		C3 P3:TAG	0.717		2	2.832		2	8.976		4
		P6:TTCA			1			3			5
EnQBCEA-MPM	$(m \leq C)$	C P:ATG	0.024	3,661	1	0.099	4,422	5	0.907	7,478	11
		C1 P1:TA	0.037	4,130	10	0.147	6,447	19	0.895	15,719	42
		C2 P2:TAG	0.026		2	0.127		2	0.886		4
		C3 P3:TGAC	0.022		1	0.102		1	0.813		1
	$(m > C)$	C1 P1:TA	0.061	4,242	10	0.264	6,606	19	1.641	16,184	42
		P4:TTC			3			9			14
		C2 P2:TC	0.047		8	0.215		20	1.585		29
		P5:TGAC			1			1			1
		C3 P3:TAG	0.051		2	0.259		2	1.883		4
		P6:TTCA			1			3			5

desired number of search iterations. Evaluating parameters No. of CIP & No. of IIP are also evaluated separately on each core. Throughout our experimentation, including exceptional cases, we measured our search results with high probability and with relative Error % value.

- We performed the repeated execution of Exact-QC and Approx.-QC for some patterns of equal size {TAA, TAG, TGA} and unequal size {TA, TAG, TGAC} on individual quantum core to analyze $(m \leq C)$ and $(m > C)$ cases. So our analysis confirms to obtain the desired values of t on different cores, based on majority, and thus the number of GSO iterations also remains same. However for these cases, based on the evaluating parameters No. of CIP and No. of IIP, the resulting outcomes of EnQPBEA and EnQBCEA algorithms were measured with either the similarity or with slight variations.
- Practically, based on values of t for Exact-QC and Approx.-QC we coded $\pi/4 \left(\sqrt{N/t} \right)$ number of GSO iterations in the searching phase of EnQPBEA and EnQBCEA algorithms. There exist some deviations in the estimated value of t through Approx.-QC algorithm. So based on this t value, if $\pi/4 \left(\sqrt{N/t} \right)$ iterations (rounded off to the nearest integer) remains same as by taking the t value through Exact-QC method, then we identify the same GSO iterations experimentally in both cases. However, the evaluating

parameters No. of CIP and No. of IIP were measured with either the similarity or with slight variations.

- On comparing the results between EnQPBEA and EnQBCEA algorithms, we observed the results of EnQPBEA as consistent and mapped with the theoretical analysis. However, there are two possible factors which are affecting the pattern searching results of EnQBCEA such as – (1) A superposition of the filtered indices (reduced search space of size $t \ll N$) are formed with $\lceil \log_2 t \rceil = tq$ qubits and this expands a search space of $O(2^{tq})$ where $tq \leq n$. Thus, if the indices $< 2^{tq}$ then we have a possibility of getting less accurate results as the number of unmarked items are comparatively more in this case. (2) With the reduced search space of size t there exist a possibility of actual pattern occurrences $t' \cong t/2$ (approximately equal to half). In this case, GSO iterations used in EnQBCEA algorithms will realize the problem of balanced function *i.e.* the pattern occurrence may be checked on the random selection of index from filtered indices. Therefore, the probability of measuring the search result would remain approximately uniform, and it actually generates less accurate results. And in the same exceptional cases, the Error % can also be observed as more.
- Based on evaluation parameters No. of CIP and No. of IIP the search results of EnQBCEA are obtained well than the EnQPBEA algorithm because of the searching is performed on the filtered indices (reduced search space) rather than the entire available search space which is used by the EnQPBEA algorithm. However, on processing overlapped pattern $\{P_2 = TTT\}$ for $(m > C)$ case, we noted the worst outcome of quantum approximate filtering (QAF). Tables 11–13 are showing the improvement in the obtained results. Therefore, in the hypothetical assumption, we may expect the search results of EnQBCEA algorithm with less Error % than the search results of EnQPBEA algorithm.

Analysis of experimental results obtained during QuEST simulation:

- For our algorithms EnQPBEA-MPM and EnQBCEA-MPM, Tables 17 and 18 are used to categorize the results between separate text file sizes $\{128, 256, 512\}$ and analysis cases $(m \leq C)$ and $(m > C)$ formed for the equal – unequal sized multiple pattern set $P = \{P_1, P_2, P_3, P_4, P_5, P_6\}$ of lengths $\{3, 3, 3, 3, 3, 3\}$ and $\{2, 2, 3, 3, 4, 4\}$. A QPU with quantum cores $C = \{C_1, C_2, C_3\}$ is considered for the separate execution of desired pattern search.
- Tables 17 and 18 includes observation on the Avg. ET (Average Execution Time of Searching), CRAM-WS (Classical RAM Workspace), and No. of IP (Number of Identified Patterns) which are mapped to the observed outcomes of Exact-QC (Exact Quantum Counting) algorithm, see Tables 11–16. We evaluated these parameters for the existing QPBE and QBCE algorithms. So, a single pattern P of length $\{3\}$ is executed on single core to simulate the case $((m = 1) < (C = 3))$. In this case, other cores are remaining idle.
- The case $((m = 3) = (C = 3))$ is considered for searching a desired pattern on individual quantum core. So, Avg. ET is separately noted, but the CRAM workspace is

noted for entire execution as the memory is shared among all cores. We used to realize $((m = 6) > (C = 3))$ for the performance evaluation with large no. of patterns (exactly doubled), and these patterns are executed on the constant number of quantum cores.

- A Avg. ET was observed using C-Library based `clock()` function call. It returns several clock ticks since the initiation of QuEST program execution. However, the clock ticks are dependent on processor architecture. So to note a time in seconds, we divide the clock ticks by `CLOCKS_PER_SEC`. This observation is noted through the test log. A CRAM workspace is observed explicitly by using process explorer to measure the maximum peak of the classical memory throughout the execution of the QuEST program.
- Our experiments for the pattern searching was repeated 20 times in a sequence to note their Avg. ET in seconds. The measured time includes the time of quantum superposition realized using ANF to simulate quantum operations in parallel.
- Both EnQPBEA and EnQBCEA are found exact for searching the pattern on target indices original or filtered text. The results tested on the dataset within QuEST simulations are here validated. Algorithms identify all pattern occurrences with high probability and in less time of execution. However, the search results of EnQBCEA are found optimal due to the search is performed on filtered space of size t rather than the original space of size N . Even on a single core, these results are optimized because of the same pattern is searched over the filtered text.
- The algorithms' performance observed in proportional increase with Avg. ET of searching, concerning the increase in text file sizes. We have stated earlier that our intentions are not to analyze the simulation efficiency due to performance restrictions on the classical machine. However, we ensure that for our text file sizes and patterns the time needed by a real quantum machine will be negligible. Average times noted for algorithms are specified explicitly for each core; but, due to parallel realization on the quantum multicore concept, we consider a maximum time taken by any core among C-QCore.
- Due to small-sized equal or unequal pattern lengths, the Avg. ET observed for both these algorithms are analyzed in close proximity. However, all the occurrences of each pattern are reported either within the original or filtered text sequence (see tables). For a case of $(m > C)$ we distributed uniform workload on all the quantum cores under the multiple (three) quantum system containing a separate register set. [Tables 17](#) and [18](#) shows proportional increase in the Avg. ET values as per the increase in file sizes. And in the same case, Avg. ET of the EnQBCEA algorithm is found optimal than the EnQPBEA algorithm.
- The search time is dependent on the size of the text sequence and the number of occurrences to report for each pattern; therefore, we consider slight deviations. For all file sizes, and the equal or unequal sized patterns, we noted the Avg. ET on individual cores. Here, the time is deviating in accordance with the size and frequency of pattern occurrences within the text sequence. Some exceptions are considered here

because of implicit random increase in depth of Boolean functions used in ANF based hybrid simulation. Recall, such an implementation aspect gives us privilege to save the number of qubits required for a simulation of algorithms.

- We restate that algorithmic performance on simulation may affect due to the scaling factors associated with qubits; thus, this also increases the workspace requirement of CRAM and processing time with an exponential increase. Memory requirement is also a crucial cum critical factor that may limit the execution of QuEST specific simulated program. So, we prepared a very small-sized data processing requirement of text and pattern and observed the utilization of the CRAM workspace (in KiB) throughout the execution of QuEST program.
- In reference to Avg. ET, we noted workspace utilization of CRAM. Therefore, the specified workspace in [Tables 17](#) and [18](#) shows the average of repetitive experiments that were performed 20 times. A CRAM consumption is observed separately with respect to single pattern on single core. We noted the combined workspace for the cases ($m = C$) and ($m > C$) to search for multiple string patterns, each one runs on separate quantum core.
- This is observed throughout the execution of algorithms that, the CRAM consumption of a single core is less on comparing with multiple quantum cores sharing. We expect this under QuEST simulation because the execution environment was set to a single quantum system with assigned registers to realize a single quantum core. For EnQPBEA and EnQBCEA, and ($m = C$) case, the execution environment of QuEST was set to multiple quantum systems with their separate registers of needed qubits to realize multiple quantum cores as a simulation of physical quantum multicore machine. So, cross-comparison assures that CRAM workspace is usually more. Similarly, for ($m > C$) case, we are observing the expected increase in CRAM workspace as each quantum system can simulate the individual quantum core to execute EnQPBEA and EnQBCEA algorithms twice to complete the execution.
- A CRAM workspace will gradually increase with respect to the text file sizes. Thus, this proportional phenomenon may restrict the classical simulation of quantum behaviour for processing the large sequence databases, usually of at least exponential in size. As well as, to process a large number of multiple string pattern m on the small number of available quantum cores C , there would be an eventual increase in the size of CRAM utilization. For all the cases ($m < C$), ($m = C$) and ($m > C$) our [Tables 17](#) and [18](#) shows the proportional increase in the CRAM workspace values as per the increase in file sizes. And for same cases, CRAM workspace of the EnQBCEA algorithm is found optimal than the EnQPBEA algorithm.
- Since we observed that the CRAM utilization of EnQBCEA for their equal – unequal sized patterns are found in the close proximate regions. However, there exists much more difference in the CRAM consumptions of EnQPBEA due to the reported pattern occurrences over the original text and implicit random increase in depth of Boolean functions used in ANF.

Table 19 Applications specific detail of proposed algorithm to process biological sequences.

Quantum algorithm	Significant characteristics	Performance restrictions	Biological sequence and databases	Specific applications
EnQPBEA- MPM	<ul style="list-style-type: none"> * Suitable for processing multiple patterns in an effective manner as its design utilizes multiple cores to search for P_k on shared QMEM. * This performs exact search, thus it is more practicable for processing biological sequences efficiently. * All exact occurrence of each P_k are found through $QCore_c$ of QPU having C cores in $O((m/C)\sqrt{N})$. * Suitable to search for long length patterns either formed over $\Sigma = 4$ (DNA) or $\Sigma = 20$ (Amino Acid), as match takes $O(1)$ on QMEM. * Exponential sized text sequence is effectively search for each pattern, irrespective of text size & frequent pattern occurrence with speedup. * Sets benchmark to find multiple pattern using multicore parallelism on text with $Pr(QCore_c) \geq t_k/N$. 	<ul style="list-style-type: none"> * High probable search results may be affected on each $QCore_c$ while processing exponentially large size text with few P_k occurrences. * For large alphabet set Σ such as $\Sigma = 20$ (Amino Acid), the qubits requirement is excessively high, as of now, it is restricted, however, no limitation on quantum machine. * Search time is still dependent on c^{th} core $QCore_c$, so, core running for the unequal sized pattern with expected more frequent occurrence, degrades algorithm performance. * The average probability of search result, with N sized text & t marked index, are proportionally increased with successive measurements. * A $O(2^n)$ depth ANF circuit slows down the simulation, and thus, this affects individual $QCore_c$ output. 	<ul style="list-style-type: none"> * DNA/RNA text is searched with a long length pattern. Equal and unequal pattern length is preferred on genome sequence. A sequence database for such examples are GenBank, DDBJ, EMBL. * Search for multiple amino acid pattern in protein database with prefer able moderate length patterns. This reduces the searching overhead. Example of some database are the GenBank, DDBJ, EMBL, GenPept, PROSITE, Swiss-Prot. 	<ul style="list-style-type: none"> * DNA/RNA/Genome/ Protein sequencing. * Local and the global sequence alignments techniques, similarity detection. * Gene and genome analysis, mapping and comparison with other similar genes of same/ different organisms. * The DNA mutation, compare investigated DNA with the known sequence. * Motif finding, open reading frame search and codons matching/ recognition. * The proteogenomics mapping read maps on genomic sequence.
EnQBCEA- MPM	<ul style="list-style-type: none"> * Performs multiple patterns search on filtered text in effectively as its design utilizes the multiple cores to search for P_k on shared QMEM. * All exact occurrence of each P_k are found through $QCore_c$ of QPU having C cores in $O((m/C)\sqrt{t})$. * Exact matching is preferred over large text that may contain frequent pattern occurrence, thus, significant to process a biological sequence. * Search mechanism is effective as because of finding patterns over the reduced size text, instead original. * This algorithm is remarkable over all classical and especially existing quantum multi-pattern methods. * Each core assures to report pattern match with $Pr(QCore_c) \geq t_k/t_k$ over individual filtered text indices. 	<ul style="list-style-type: none"> * The probability of search results at k^{th} core $QCore_c$ will depend on relativeness of individual filtered indices to the occurrences of pattern present in filtered text for each P_k. * Bothe filtering and search time is still dependent on c^{th} core $QCore_c$, so, core running for unequal sized pattern with more filtering outcome and frequent search occurrence may degrades algorithm performance. * Due to algorithmic filtering, the qubits requirement increases with (m/C), thus, restricts simulation. * Performance on each $QCore_c$ is affected with unequal length pattern and its formation over large Σ. * $O(2^{tq})$ $tq \leq n$ ANF circuit depth slows down simulation, and thus, it affects individual $QCore_c$ output. 	<ul style="list-style-type: none"> * Multiple codon can code for same amino acid with either single or the multi locations within sequence. * DNA/RNA/Peptide & Protein sequences are preferably search with the small length pattern for simulation and no restrictions on quantum machine. * The biological text sequence database as can search for multi pattern. In example GenBank, Nucleotide database, PROSITE, GenPept, Swiss-Prot, DDBJ, EMBL. 	<ul style="list-style-type: none"> * DNA/RNA/Genome/ Protein sequencing. * Preferable approach for method of multiple sequence alignment. * Motif finding, open reading frame search and codons matching with using a similarity detection/checking. * Apply over specific nucleotide or peptide sequences to deal with the local alignment. * Apply to a sequence alignment (global) on genome or protein. * Applicable on gene mapping and the exact substring matching.

Our observations on QuEST specific simulation mainly involves the critical factor of qubits requirement for simulating quantum algorithm. It may cause exhaustive use of CRAM, and the classical CPU computation time is also increased with the at least exponential factor to process the circuit depth of quantum algorithms. However, we implemented quantum algorithms with hybrid simulation by effectively utilizing QuEST performance with several optimizations.

Proposed algorithmic applications to process biological sequences

This section defines several applications of our proposed quantum algorithms related to search multiple patterns within the biological sequence databases. [Table 19](#) specifies the applicability of proposed algorithms with respect to significant characteristics and performance restrictions.

- In [Table 19](#), we summarize the significant characteristics and performance restrictions of the presented algorithms. We highlighted main points with respect to the contextual interpretation of biological text sequences and their standardized databases. To have more understanding of the algorithms, we direct the reader to specific applications ([Sheik, Aggarwal & Anindya Poddar, 2004](#); [Basel, 2006](#); [Choo, 2006](#); [Kalsi, Peltola & Tarhio, 2008](#); [Fredriksson, 2009](#); [Charalampos, Panagiotis & Konstantinos, 2011](#); [Rivals, Salmela & Tarhio, 2011](#); [Faro & Lecroq, 2013](#); [Jiang, Zhang & Zhang, 2013](#); [Singh, 2015](#); [Zhang et al., 2015](#); [Tahir, Sardaraz & Ikram, 2017](#); [Hakak & Kamsin, 2019](#); [Neamatollahi, 2020](#); [Soni & Rasool, 2021](#); [Soni & Malviya, 2021](#); [Raja & Srinivasulu Reddy, 2019](#)). These articles are related to process biological sequences and their databases.
- In general, we say that the presented algorithms to process biological sequences, are influenced by three parameters such as alphabet size, pattern length and the size of the text. These parameters may affect the performance of the algorithmic simulation. However, their realization of quantum machines would be effective in specific biological applications.
- The probability of search results is based on the relativity between pattern occurrences and the size of the text database (original or filtered). Therefore, the search results are obtained in the best time with at least half probability, and for more frequent pattern occurrences, the results are obtained in the worst time with very high probability.
- In multiple pattern processing, there exist some variations in the performance of algorithm. It is because of processing equal or unequal size patterns. The simulation over a very large-sized biological sequence database is not feasible for simulation because of higher qubits requirement; therefore, a subset of the database is searched for a pattern as per the feasibility. There is no such restriction on real quantum machines as they can realize effective processing.

CONCLUSION AND FUTURE WORK

In this work, we enhanced the existing quantum pattern matching methods QPBE and QBCE to search multiple patterns in parallel by using QPU with C cores accessing text on

shared QMEM. The search time to find all occurrences of the individual patterns overlapped implicitly. Based on several complexity analysis factors, our proposed quantum algorithms EnQPBEA-MPM and EnQBCEA-MPM are proved efficient to find exact patterns while comparing with existing multiple pattern methods such as QEMP and QAMP as their quantum design cannot exclude multiplicative factor m . A design of presented algorithms uses architectural parallelism, but with a multiplicative constant m/C . This factor can be negligible for small arbitrary constant value of m and constant value of C . However, for comparatively large value of $m \gg C$, a factor m/C cannot be ignored in the time complexities. Similarly, due to an implicit operational parallelism, the logarithmic factor is found negligible when the original or filtered search space remains too small to expand in superposition. However, this logarithmic factor cannot be ignored with large number of qubits. Indeed, our proposed algorithms are preferred effectively for finding the few pattern occurrences. Therefore, to process the exponentially large size biological text sequences, our $O((m/C)\sqrt{N})$ and $O((m/C)\sqrt{t})$ time quantum solutions are efficient, and they outperform over existing classical as well as quantum solutions by achieving speedups. The algorithms are justified, based on mathematical proves, as equivalent to quantum circuits. To obtain the accurate search results, quantum counting is explicitly added to the functionality of proposed algorithms. We suggested specific applications of these algorithms related to biological sequence processing.

The quantum algorithms are validated through restricted simulation performance. We used Exact-QC to measure exact value of t and to validate the accurate search results. However, we analyzed the deviations and less accurate search results by combining Approx.-QC and GSO operator. The possible cases ($m \leq C$) and ($m > C$) were used in our experimentation to observe the variations in search results. Indeed, our intentions were not to analyze the simulation efficiency; therefore, as per the feasibility, we presented the hybrid simulation to realize quantum operations of the algorithm on the classical machine. However, we seek their efficient execution on the real quantum machine to observe the high-performance computation aspects. Further, the proposed work can be extended possibly either to replace filtering approximations of EnQBCEA with exactness or to modify this using other error metric methods to increase accuracy. The open problems would be the realizations of multiple oracles in parallel on a single quantum core, such that the multiplicative factors can be completely removed, and the design of search method through phase matching as replacement of amplitude amplification.

ACKNOWLEDGEMENTS

The authors are thankful to the domain researchers for sharing their ideas to extend over upcoming quantum technology. We are also thankful to the reviewers as their valuable suggestions improved the quality of the article.

ADDITIONAL INFORMATION AND DECLARATIONS

Funding

The authors received no funding for this work.

Competing Interests

The authors declare that they have no competing interests.

Author Contributions

- Kapil Kumar Soni conceived and designed the experiments, performed the experiments, analyzed the data, performed the computation work, prepared figures and/or tables, authored or reviewed drafts of the paper, quantum algorithm design & analysis, and writing of complexity proofs, and approved the final draft.
- Akhtar Rasool analyzed the data, authored or reviewed drafts of the paper, and approved the final draft.

Data Availability

The following information was supplied regarding data availability:

The sequences are available at Genbank: [MW687138](#).

The QuEST Simulation Codes are available at GitHub:

<https://github.com/profkapilsoni/EnQPBEA-and-EnQBCEA-Algorithms>.

Supplemental Information

Supplemental information for this article can be found online at <http://dx.doi.org/10.7717/peerj-cs.957#supplemental-information>.

REFERENCES

- Ablayev F, Ablayev M, Khadiev K, Salihova N, Vasiliev A. 2020.** Quantum algorithms for string processing. Available at <https://arxiv.org/abs/2012.00372>.
- Aborot J. 2017.** Quantum approximate string matching for large alphabets. *Theory & Practice of Computation* 1:37–50 DOI [10.1142/10334](https://doi.org/10.1142/10334).
- Basel B. 2006.** Biological sequences and the exact string matching problem. In: *Introduction to Computational Biology*. 43–63.
- Bogdanova YI, Bogdanova NA, Fastovets DV, Lukichev VF. 2018.** Representation of Boolean function in terms of quantum computations. Available at <http://arxiv.org/abs/1906.06374>.
- Boyer M, Brassard G, Hoyer P, Tapp A. 1998.** Tight bounds on quantum searching. *Fortschritte der Physik* 46(4–5):493–505
DOI [10.1002/\(SICI\)1521-3978\(199806\)46:4/5<493::AID-PROP493>3.0.CO;2-P](https://doi.org/10.1002/(SICI)1521-3978(199806)46:4/5<493::AID-PROP493>3.0.CO;2-P).
- Brandl MF. 2017.** A quantum von Neumann architecture for large scale quantum computing. Available at <http://arxiv.org/abs/1702.02583>.
- Brassard G, Hoyer P, Mosca M, Tapp A. 2002.** Quantum amplitude amplification and estimation. *Contemporary Mathematics* 305:53–74 DOI [10.1090/conm/305/05215](https://doi.org/10.1090/conm/305/05215).
- Britt KA. 2017.** High performance computing with quantum processing units. *ACM Journal on Emerging Technologies in Computing System* 13(39):1–13 DOI [10.1145/3007651](https://doi.org/10.1145/3007651).
- Broda B. 2016.** Quantum search of a real unstructured database. *European Physics Journal Plus* 131(38):1–4 DOI [10.1140/epjp/i2016-16038-2](https://doi.org/10.1140/epjp/i2016-16038-2).
- Chakrabarty I, Khan S, Singh V. 2017.** Dynamic Grover search: application in recommendation system & optimization problems. *Quantum Information Processing* 16(6):152–172
DOI [10.1007/s11128-017-1600-4](https://doi.org/10.1007/s11128-017-1600-4).

- Charalampos S, Panagiotis D, Konstantinos G. 2011.** Parallel processing of multiple pattern matching algorithms for biological sequences: methods and performance results. In: *Bioinformatics–Computational Biology and Modeling*. Intech, 161–182 DOI [10.5772/18488](https://doi.org/10.5772/18488).
- Choo KW. 2006.** Quantum computing: Grover’s search algorithm and its applications in bioinformatics. *COSMOS World Scientific* **2(1)**:71–80 DOI [10.1142/S0219607706000171](https://doi.org/10.1142/S0219607706000171).
- Coles PJ. 2020.** Quantum algorithm implementations for beginners. Available at <http://arxiv.org/abs/1804.03719v2>.
- De Jesus BKA, Aborot JA, Adorna HN. 2013.** Solving the exact pattern matching problem constrained to single occurrence of pattern P in string S Using Grover’s quantum search algorithm. In: *Theory & Practice of Computation, Proceedings in Information & Communications Technology Springer*. Vol. 7. 124–142.
- Faro S, Lecroq T. 2009.** An efficient matching algorithm for encoded DNA sequences and binary strings. *LNCs Springer* **5577**:106–115 DOI [10.1007/978-3-642-02441-2](https://doi.org/10.1007/978-3-642-02441-2).
- Faro S, Lecroq T. 2013.** The exact online string matching problem: a review of the most recent results. *ACM Computing Surveys* **45(2)**:1–42 DOI [10.1145/2431211.2431212](https://doi.org/10.1145/2431211.2431212).
- Figgatt C, Maslov D, Landsman KA, Linke NM, Debnath S, Monroe C. 2017.** Complete 3-qubit Grover search on a programmable quantum computer. *Nature Communications* **8(1)**:1918 DOI [10.1038/s41467-017-01904-7](https://doi.org/10.1038/s41467-017-01904-7).
- Fredriksson K. 2009.** Succinct backward-DAWG-matching. *ACM Journal of Experimental Algorithmics* **13(8)**:1.1–1.26 DOI [10.1145/1412228.1455263](https://doi.org/10.1145/1412228.1455263).
- Fu X, Riesebo L, Lao L, Almudever CG, Sebastiano F, Versluis R, Charbon E, Bertels K. 2016.** A heterogeneous quantum computer architecture. In: *Proceedings of the ACM CF – 16 International Conferences on Computing Frontiers*. 323–330.
- Giovannetti V, Lloyd S, Maccone L. 2008.** Quantum random access memory. *Physics Review Letters* **100(16)**:1–4 DOI [10.1103/PhysRevLett.100.160501](https://doi.org/10.1103/PhysRevLett.100.160501).
- Giri PR, Korepin VE. 2017.** A review on quantum search algorithms. *Quantum Information Processing* **16(12)**:315 DOI [10.1007/s11128-017-1768-7](https://doi.org/10.1007/s11128-017-1768-7).
- Grassi L, Plasencia MN, Schrottenloher A. 2018.** Quantum algorithms for the k-xor problem. In: *Advances in Cryptology – ASIACRYPT*. Berlin: Springer, 527–559.
- Hakak SI, Kamsin A. 2019.** Exact string matching algorithms—survey, issues, and future research directions. *IEEE Access* **7**:69614–69637 DOI [10.1109/ACCESS.2019.2914071](https://doi.org/10.1109/ACCESS.2019.2914071).
- Hao X, Zhang F, Xia S, Zhou Y. 2020.** Quantum algorithms for learning the algebraic normal form of quadratic Boolean functions. *Quantum Information Processing* **19(273)**:1–22 DOI [10.1007/s11128-020-02778-3](https://doi.org/10.1007/s11128-020-02778-3).
- Hendrian D, Ueki Y, Narisawa K, Yoshinaka R, Shinohara A. 2019.** Permuted pattern matching algorithms on multi-track strings. *Algorithms MDPI Journal* **12(4)**:1–20 DOI [10.3390/a12040073](https://doi.org/10.3390/a12040073).
- Jiang R, Zhang X, Zhang MQ. 2013.** *Basics of bioinformatics, lecture notes of the graduate summer school on bioinformatics of China*. Beijing: Springer and Tsinghua University Press.
- Jones T, Benjamin C. 2018.** QuEST and high performance simulation of quantum computers. *Science Reports* **9(1)**:1–9 DOI [10.1038/s41598-019-47174-9](https://doi.org/10.1038/s41598-019-47174-9).
- Kalsi P, Peltola H, Tarhio J. 2008.** Comparison of exact string matching algorithms for biological sequences. *CCIS Springer* **13**:417–426 DOI [10.1007/978-3-540-70600-7](https://doi.org/10.1007/978-3-540-70600-7).
- Lanzogorta M, Uhlmann J. 2008.** Quantum computer science. *Synthesis Lectures on Quantum Computing* **1(1)**:1–124 DOI [10.2200/S00159ED1V01Y200810QMC002](https://doi.org/10.2200/S00159ED1V01Y200810QMC002).

- Lin C-H, Liu C-H, Chien L-S, Chang S-C. 2013.** Accelerating pattern matching using a novel parallel algorithm on GPUs. *IEEE Transaction on Computers* **62(10)**:1906–1916 DOI [10.1109/TC.2012.254](https://doi.org/10.1109/TC.2012.254).
- Lomont C. 2003.** Robust string matching in $O(\sqrt{N} + M)$ quantum queries. Available at <https://arxiv.org/abs/quant-ph/0311043v2>.
- Malviya AK, Tiwari N. 2020.** Linear approximation of a vectorial Boolean function using quantum computing. *Europhysics Letters* **132(4)**:40001 DOI [10.1209/0295-5075/132/40001](https://doi.org/10.1209/0295-5075/132/40001).
- Malviya AK, Tiwari N. 2021.** Quantum algorithm to identify division property of a multiset. *Arabian Journal of Science and Engineering* **46(9)**:8711–8719 DOI [10.1007/s13369-021-05665-w](https://doi.org/10.1007/s13369-021-05665-w).
- Matteo OD. 2020.** Fault tolerant resource estimation of quantum random access memories. *IEEE Transaction on Quantum Engineering* **1**:1–13 DOI [10.1109/TQE.2020.2965803](https://doi.org/10.1109/TQE.2020.2965803).
- Menon V, Chattopadhyay A. 2021.** Quantum pattern matching oracle construction. *Pramana – Journal of Physics* **95(1)**:22 DOI [10.1007/s12043-020-02062-0](https://doi.org/10.1007/s12043-020-02062-0).
- Metodi TS. 2011.** *Quantum computing for computer architects*. Second Edition. San Rafael: Morgan & Claypool Publishers.
- Montanaro A. 2017.** Quantum pattern matching fast on average. *Springer Journal Algorithmica* **77(1)**:16–39 DOI [10.1007/s00453-015-0060-4](https://doi.org/10.1007/s00453-015-0060-4).
- Neamatollahi P. 2020.** Simple and efficient pattern matching algorithms for biological sequences. *IEEE Access* **8**:38–46 DOI [10.1109/ACCESS.2020.2969038](https://doi.org/10.1109/ACCESS.2020.2969038).
- Nielsen MA, Chuang IL. 2010.** *Quantum computation and quantum information*. Tenth Edition. Cambridge: Cambridge University Press.
- Park DK, Petruccione F. 2019.** Circuit-based quantum random access memory for classical data. *Quantum Physics, Scientific Reports* **9(1)**:1–8 DOI [10.1038/s41598-019-40439-3](https://doi.org/10.1038/s41598-019-40439-3).
- Raja G, Srinivasulu Reddy U. 2019.** Maximum exact matches for high throughput genome subsequence assembly. *IETE Journal of Research* **3(1)**:1–8 DOI [10.1080/03772063.2019.1603085](https://doi.org/10.1080/03772063.2019.1603085).
- Ramesh H, Vinay V. 2003.** String matching in $O(\sqrt{n} + \sqrt{m})$ quantum time. *Journal of Discrete Algorithms* **1(2)**:103–110 DOI [10.1016/S1570-8667\(03\)00010-8](https://doi.org/10.1016/S1570-8667(03)00010-8).
- Rivals E, Salmela L, Tarhio J. 2011.** Exact search algorithms for biological sequences. In: *Algorithms in Computational Molecular Biology - Techniques, & Applications*. John Wiley & Sons, 91–111.
- Sena Oliveira D, Benicio Melo de Sousa P, Viana Ramos R. 2007.** Quantum bit string comparator —circuits and applications. *IEEE International Telecommunications Symposium* **7**:17–26 DOI [10.1109/ITS.2006.4433341](https://doi.org/10.1109/ITS.2006.4433341).
- Sheik SS, Aggarwal SK, Anindya Poddar NB. 2004.** A fast pattern matching algorithm. *Journal of Chemical Information and Computer Science* **44(4)**:1251–1256 DOI [10.1021/ci030463z](https://doi.org/10.1021/ci030463z).
- Singh GB. 2015.** *Fundamentals of bioinformatics and computational biology*. Vol. 6. Cham: Springer International Publishing Switzerland, 1–345.
- Song F. 2017.** Early days following Grover’s quantum search algorithm. Available at <http://arxiv.org/abs/1709.01236>.
- Soni B, Khare N, Soni KK, Rasool A. 2020.** Classical equivalent quantum based efficient data preprocessing algorithm. In: *IEEE International Conference on Computing, Communication and Networking Technologies (ICCCNT)*. Piscataway: IEEE.
- Soni KK, Malviya AK. 2021.** Design and analysis of pattern matching algorithms based on QuRAM processing. *Arabian Journal for Science and Engineering* **46(4)**:3829–3851 DOI [10.1007/s13369-020-05310-y](https://doi.org/10.1007/s13369-020-05310-y).

- Soni KK, Rasool A. 2020.** Pattern matching: a quantum oriented approach. *Procedia Computer Science* **167(1)**:1991–2002 DOI [10.1016/j.procs.2020.03.230](https://doi.org/10.1016/j.procs.2020.03.230).
- Soni KK, Rasool A. 2021.** Quantum-based exact pattern matching algorithms for biological sequences. *ETRI Journal* **46(3)**:483–510 DOI [10.4218/etrij.2019-0589](https://doi.org/10.4218/etrij.2019-0589).
- Tahir M, Sardaraz M, Ikram AA. 2017.** EPMA: efficient pattern matching algorithm for DNA sequences. *Expert Systems with Applications* **80**:161–170 DOI [10.1016/j.eswa.2017.03.026](https://doi.org/10.1016/j.eswa.2017.03.026).
- Younes A. 2008.** Strength and weakness in Grover’s quantum search algorithm. Available at <https://arxiv.org/abs/0811.4481>.
- Zhang H, Xu D, Tian Z, Fan Y. 2015.** An efficient parallel algorithm for exact multi-pattern matching. *Security and Communication Networks* **8(9)**:1688–1697 DOI [10.1002/sec.1115](https://doi.org/10.1002/sec.1115).
- Zhou Q, Lu S, Zhang Z, Sun J. 2015.** Quantum differential cryptanalysis. *Quantum Information Processing* **14(6)**:2101–2109 DOI [10.1007/s11128-015-0983-3](https://doi.org/10.1007/s11128-015-0983-3).
- Zhou R-G, Shen C-Y, Xiao T-R, Li Y-C. 2013.** Quantum pattern search with closed match. *International Journal of Theoretical Physics* **52(11)**:3970–3980 DOI [10.1007/s10773-013-1710-4](https://doi.org/10.1007/s10773-013-1710-4).
- Zou D, Ma L, Yu J, Zhang Z. 2015.** Biological databases for human research. *Genomics Proteomics Bioinformatics* **13(1)**:55–63 DOI [10.1016/j.gpb.2015.01.006](https://doi.org/10.1016/j.gpb.2015.01.006).